Asian Journal of Electrical and Electronic Engineering

VOLUME 2 ISSUE 1 MARCH 2022

eISSN 2785-8189

https://alambiblio.com/ojs/index.php/ajoeee

ASIAN JOURNAL OF ELECTRICAL AND ELECTRONIC ENGINEERING

AIMS & SCOPE OF THE ASIAN JOURNAL OF ELECTRICAL AND ELECTRONIC ENGINEERING

The **Asian Journal of Electrical and Electronic Engineering** (**AJoEEE**), published biannually (March and September), is a peer-reviewed open-access journal of the **AlamBiblio Press**.

The Asian Journal of Electrical and Electronic Engineering publishes original research findings as regular papers and review papers (by invitation). The Journal provides a platform for Engineers, Researchers, Academicians, and Practitioners who are highly motivated to contribute to the Electrical and Electronics Engineering disciplines. It also welcomes contributions that address the developing world's specific challenges and address science and technology issues from a multidisciplinary perspective.

REFEREES' NETWORK

All papers submitted to AJoEEE Journal will be subjected to a rigorous reviewing process through a worldwide network of specialized and competent referees. Each accepted paper should have at least two positive referees' assessments.

SUBMISSION OF A MANUSCRIPT

A manuscript should be submitted online to the Asian Journal of Electrical and Electronic Engineering (AJoEEE) website https://alambiblio.com/ojs/index.php/ajoeee. Further correspondence on the status of the paper could be done through the journal website

COPYRIGHT NOTICE

Consent to publish: The Author(s) agree to publish their articles with AlamBiblio Press.

Declaration: The Author(s) declare that the article has not been published before in any form. It is not concurrently submitted to another publication, and it does not infringe on anyone's copyright. The author (s) holds the AlamBiblio Press and Editors of the Journal harmless against all copyright claims.

Transfer of copyright: The Author(s) hereby agrees to transfer the article's copyright to AlamBiblio Press, which shall have the non-exclusive and unlimited right to publish the article in any form, including electronic media. For the article with more than one author, the corresponding author confirms that he/she is authorised by his/her co-author(s) to grant this transfer of copyright.

The Asian Journal of Electrical and Electronic Engineering journal follows the open access policy.

All articles published with open access will be immediately and permanently free for everyone to read, download, copy, distribute, and be NonCommercial.

ASIAN JOURNAL OF ELECTRICAL AND ELECTRONIC ENGINEERING

eISSN 2785-8189

9 772785 818002

Published by:

AlamBiblio Press,
PV8 platinum Hill
Jalan Melati Utama, 53100 Kuala Lumpur, Malaysia
Phone (+603) 2713 7308

ASIAN JOURNAL OF ELECTRICAL AND ELECTRONIC ENGINEERING

Volume 2, Issue 1, March 2022

TABLE OF CONTENTS

ASIAN JOURNAL OF ELECTRICAL AND ELECTRONIC ENGINEERING
Vol. 2 No. 1 2022
E-ISSN: 2785-8189

Analysis of blockchain-based Ripple and SWIFT

Md Rafiqul Islam[1*], Muhammad Mahbubur Rashid[2], Mohammed Ataur Rahman[3], Muslin Har Sani Bin Mohamad[4], Abd Halim Bin Embang[5]

[1]*Department of Mechatronics, Faculty of Engineering, International Islamic University Malaysia*
[2]*Department of Mechatronics, Faculty of Engineering, International Islamic University Malaysia*
[3]*Department of Mechanical Engineering, International Islamic University Malaysia*
[4]*Department of Accounting, International Islamic University Malaysia*
[5]*Department of Mechatronics, Faculty of Engineering, International Islamic University Malaysia*

*Corresponding author: engrrafiqul@gmail.com

(Received:24th January 2022; Accepted: 28th February 2022)

Abstract— Blockchain is one of the modern new edge technologies which is capable of transforming the traditional financial system, especially in the financial industry. Cross-border money transfer is one of the big challenges in terms of security, cost, and other regulatory issues. Presently, the most popular international money transfer system is SWIFT in the financial sector. Ripple is one of the upcoming payment networks for cross-border payment systems based on blockchain technology and uses its own cryptocurrency called XRP. This paper highlights the implementation challenges of SWIFT and Ripple networks. It also underlines the features of whether the blockchain-based application can transform the existing traditional payment system and how the new proposed system works. This paper is also explained how the proposed system has some advantages over the traditional system. Still, SWIFT is the market leader in remitting money for cross-border payments. On the other hand, the Ripple network is an emerging technology that may contribute a lot to cross-border payment in the financial industry in the near future.

Keywords: *Blockchain, SWIFT, Ripple, XRP, Cryptocurrency*

1. INTRODUCTION

Society for Worldwide Interbank Financial Telecommunications (SWIFT) was founded in 1973, where participants were 239 banks in 15 countries. In the year 2021, SWIFT has been processed an average of 42.5 million messages per day [1]. Before implementing the SWIFT service for cross-border payments, the remittance system called Telex was used in the financial industries. SWIFT introduced the standard fixed-size code called SWIFT code, through which the remittance operation has become user-friendly and more authentic [2]. Most of banks are using SWIFT across the globe.

The telex machine is very similar to the typewriter machine that is connected to the printer, where the data is transmitted from the telex machine to another telex machine through a telephonic circuit [3]. The Telex system was used for domestic as well as international money transfer purposes. The free-form message formats were used by the telex machine.

Though SWIFT is very popular, there are still huge liquidity and credit risks that exist in the SWIFT network in financial institutes. Another remarkable drawback is a third-party dependency which may accelerate the fraudulent activity. Clearing settlement or reconciliation unit needs to maintain separately in both ends sender and receiver institute.

On the other hand, the Ripple network has been developed based on blockchain technology which eliminates the intermediator between the sender and receiver banks. The sender bank can make the cross-border payment directly to the beneficiary's bank account without any delay [4]. The blockchain application system maintains the authenticity of the payment by using distributed ledger technology, and the transaction process is completed by using their own digital token or cryptocurrency [5]. Here Ripple is using their own digital currency called XRP.

It works as a digital medium that allows the conversion of the different currencies to XRP [6]. All the transactional data, reconciliation, and settlement are completed instantly in the Ripple network [7]. Transaction in the Ripple network is not possible until synchronizing all the transactional data. Ripple network is very secure and cost-effective, and no additional settlement time is required to complete the whole transactional data in both sender and receiver banks [8].

Though SWIFT is a very renowned cross-border payments platform in the market, the Ripple system has also become an emerging payment network platform due to its reliability, cost-effectiveness, and support for the real-time settlement process, which may replace the traditional SWIFT system. The originality of this paper analyses the core technical functions of SWIFT and Ripple as well as highlights the challenges for the same. This paper also helps the new researcher to work on blockchain-based application systems in the financial sector.

2. SWIFT MONEY TRANSFER SYSTEM

SWIFT system is used to transfer money domestically and internationally among the member institutes of its' network. It is a member-owned cooperative and ensures a safe and secure platform to transfer money. All member institutions are working under a SWIFT network to ensure their identities and all members are holding the unique institution ID number [9]. SWIFT always uses predefined code to send the messages from sender to receiver institute. The SWIFT standard code maintains 4 components called bank code four digits, country code 2 digits, location code 2 digits, and 3 digits for the bank's branch code [10]. For example, the SWIFT code is BCOLBDDHXXX. The first four-digit BCOL is used for bank identification which represents the Bengal Commercial Bank Limited, the next two-digit BD represents the country code for Bangladesh, the third component which consists of 2 digits DH is used to identify the location of Dhaka, and the final three-digit XXX represents the branch code of the bank. The branch code XXX is optional and is used only for the bank's internal purpose of identifying the branch. The other parts of the message body follow the specific SWIFT message format for representing the universal message format. SWIFT can send messages only from one member to another. There are two parts to the SWIFT system: message transfer and payment settlement instruction [11]. The payment settlement instructions are executed at the bank's end. Several standard SWIFT message formats are used to send the message from sender to receiver institution.

2.1 Message Transfer Process

SWIFT message transfer instruction is explained in Fig. 1 below. All the messages are prepared as per SWIFT standard format by the sender. It is sent to the SWIFT network for making the payments to the receiver and other related information as well. For all the messages sent from one country to another country for cross-border payment, SWIFT convert all the message as per their valid standard message format. SWIFT networks not only check the standard format, but they also do the message through a sanction screening software for authentication of the sender and receiver. The message sends by the SWIFT network to the receiver end and one copy is sent back to the sender end for checking the delivery authenticity. Finally, the receiver checks all the payment's instruction validity and contacts the beneficiary of the payment, but the sender gets the latest report on the entire process.

2.2 Payment Settlement Process

The payment settlement process is conducted at the respective bank end and this process is dependent on their procedure. SWIFT payment follows a few numbers of steps. First, the payment originator conducted with his/her bank which is called the originating bank. The originating bank then conducts with the corresponding bank for transferring the cross-border payment to the beneficiary's bank account. The originating bank communicates with the central bank for currency conversion or currency exchange. The central bank then helps to transfer the money from the central bank to the corresponding bank. Finally, the money transferred to the beneficiary's bank account number of the beneficiary's bank account. The corresponding banks for sender and receiver deduct the charges for the transactions. All the corresponding payment instructions follow the standard SWIFT message format, and all the messages are stored in all the above entities, which are verified by sanctioned screening and other international and domestic regulatory requirements. The sender has also updated the entire process.

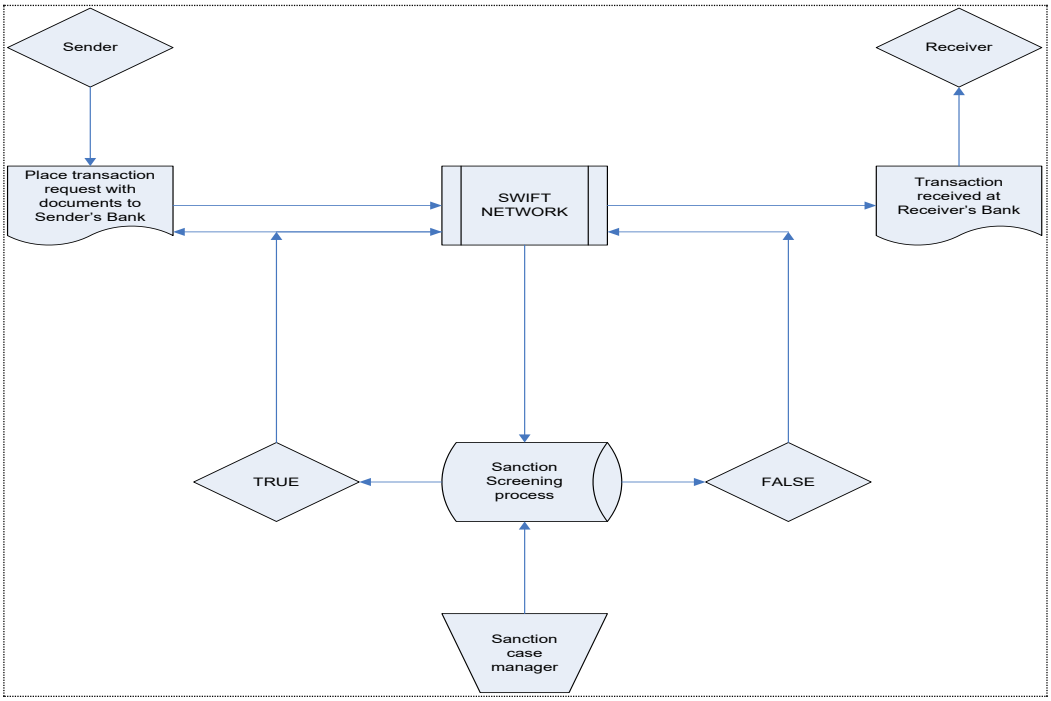

Fig. 1: SWIFT Message Process Flowchart

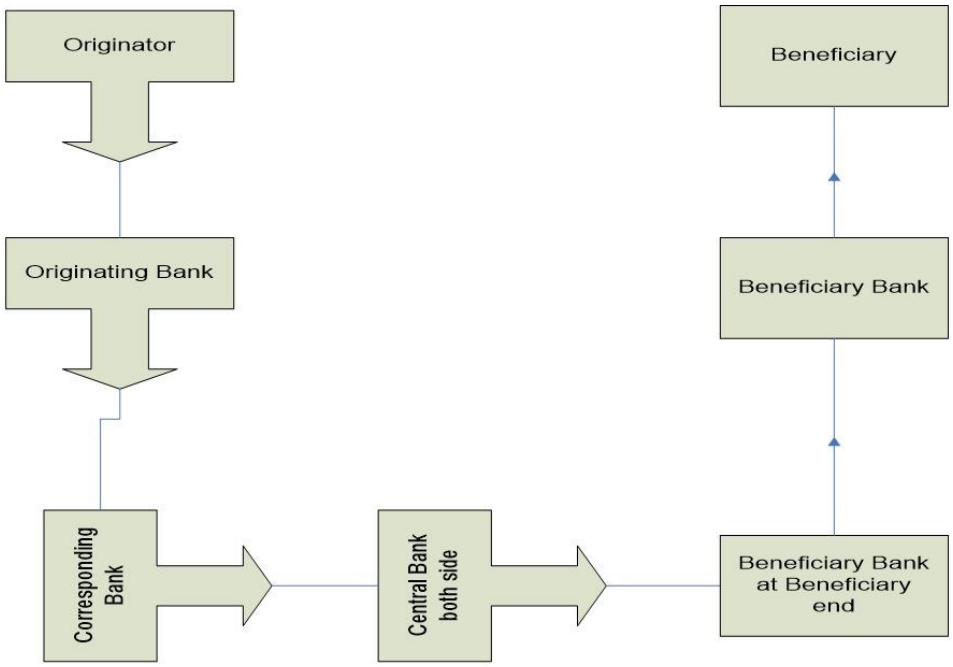

Fig. 2: SWIFT Payment Settlement Process

As per the above diagram (fig.1 and Fig.2), the SWIFT message transfer flow and settlement process are involved in several steps. But the fund transfer process can be conducted among the several banks in the SWIFT network. The fund transfer or payment can be stopped at any stage if there is any liquidity problem with the bank. In that case, it will take a significant amount of time to complete the settlement process. It means that the transaction process through SWIFT is not synchronized or real-time. On the other hand, the settlement process is taking longer and is less cost-effective.

2.3 SWIFT Implementation Challenges

i) Technology adaptation

Before implementing the SWIFT application in the financial institute, the implementation team should have a full understanding of the business need and must have a clear understanding of SWIFT operational process flows. Selecting the SWIFT implementation partner is another challenge than hiring talents from the industries.

ii) Secure Network setup

Secured Network setup is a very big challenge which is one of the mandatory requirements by the SWIFT organization. SWIFT network should be installed as per their guideline which is challenging and costly as well. This network should be isolated from the other network of the bank, must have deployed the two-factor authentication system, and must follow the SWIFT message formats and other instructions.

iii) Maintenance

SWIFT changes its requirements from time to time which needs to implement promptly to comply with them. They also provide the patches regularly that must have to upload in the SWIFT application. All these changes should be uploaded before doing any transaction in the network.

iv) Anti-Money Laundering (AML)

Nowadays, the AML issue is one of the biggest concerns for financial institutions and regulatory bodies as well. They have strictly followed the regulatory compliance to protect the criminal financing and illegal cross-border money transfer. Before making any payment, the financial institute should sanction the Transaction for cross-border payment and should verify the Know Your Customer (KYC).

v) Intermediator

SWIFT works as an intermediator for making cross-border payments from one country to another. Payment initiators or remitters cannot make payments directly to the beneficiary's account. So, it takes time, and the remitter needs to pay SWIFT transaction fees and other fees to the bank. Security is another big concern in this payment method.

vi) Reconciliation

SWIFT operation is not synchronized. As a result, real-time reconciliation is not possible with this network. IT is a time-consuming and hard job for the banks to run the settlement process due to the huge amount of data. Sometimes banks cannot complete the reconciliation process on time and the Cash flow management becomes very difficult with unreconciled data in the financial institutes.

3. RIPPLE NETWORK

Blockchain is one of the modern technologies which can be used to develop blockchain-based applications for cross-border payment. Ripple is one of the blockchain-supported networks for international cross-border payment. Two features of blockchain technology called Distributed Ledger (DL) and Cryptocurrency are used in Ripple [12]. All the transactions in the Ripple network are real-time, so it transfers the message and fund transfer instructions together [13]. But in the SWIFT operation, the message transfer process and fund transfer process are not synchronized. Ripple uses cryptocurrency tokens that support converting all other currencies to a single currency called XRP. Ripple also uses blockchain distributed ledger technology to pass the Transaction on the Peer-to-Peer (P2P) network [14]. All transactional information and settlement in the Ripple network would be completed immediately once the payment transaction initiates by the sender. Both the messaging and settlement features are exit the Ripple network. Transaction for cross-border payment through the Ripple network is faster than SWIFT. Within a few seconds, payment can be credited to the beneficiary's account and at the same time, settlement is also real-time. So, the cost to transfer the money through Ripple is much cheaper than SWIFT.

The blockchain concept was first introduced by a pseudonymous person or a group of persons called Satoshi Nakamoto in 2009 [15]. Blockchain is a technology that represents the data as a chain of blocks that gather the data in the blocks. It is a list-type data structure, immutable data structure, and cryptographically chains block in chronological order [16]. Each block contains data, the previous block hash value (The first block of a blockchain

contains the initial value, which is '0000'), timestamp, and the transaction data. The previous block hash is the initial hash of the current block. Cryptographic hashing algorithm and digital signature have ensured the consistency of data. Once the data send by the sender, it is not possible to alter the data in the blockchain network. Always blockchain network generates new blocks by solving the mathematical puzzle, and at the same time, all the connected nodes in the network will be updated accordingly. All the consensus protocols in the P2P blockchain network update and validate the newly generated blocks.

Ripple is always maintaining the currency conversion rate among the consortium or member banks. The Ripple network is very transparent to provide the liquidity status of the sender bank; on the other hand, SWIFT can provide the minimum liquidity information of the sender bank.

All corporate and retail customers look for a low-cost solution for making their cross-border payments as well as demand for real-time payment. Still, there are some limitations on the bank's infrastructure and banks are bound to process the payment in batch, with high processing costs and lengthy settlement time.

To address the above, the Ripple application provides an open-ended, neutral protocol called Inter Ledger Protocol (ILP) which brings an efficient, faster, real-time settlement process that removes the settlement risks. Four components help to complete the entire Transaction between sender and receiver for cross-border payment.

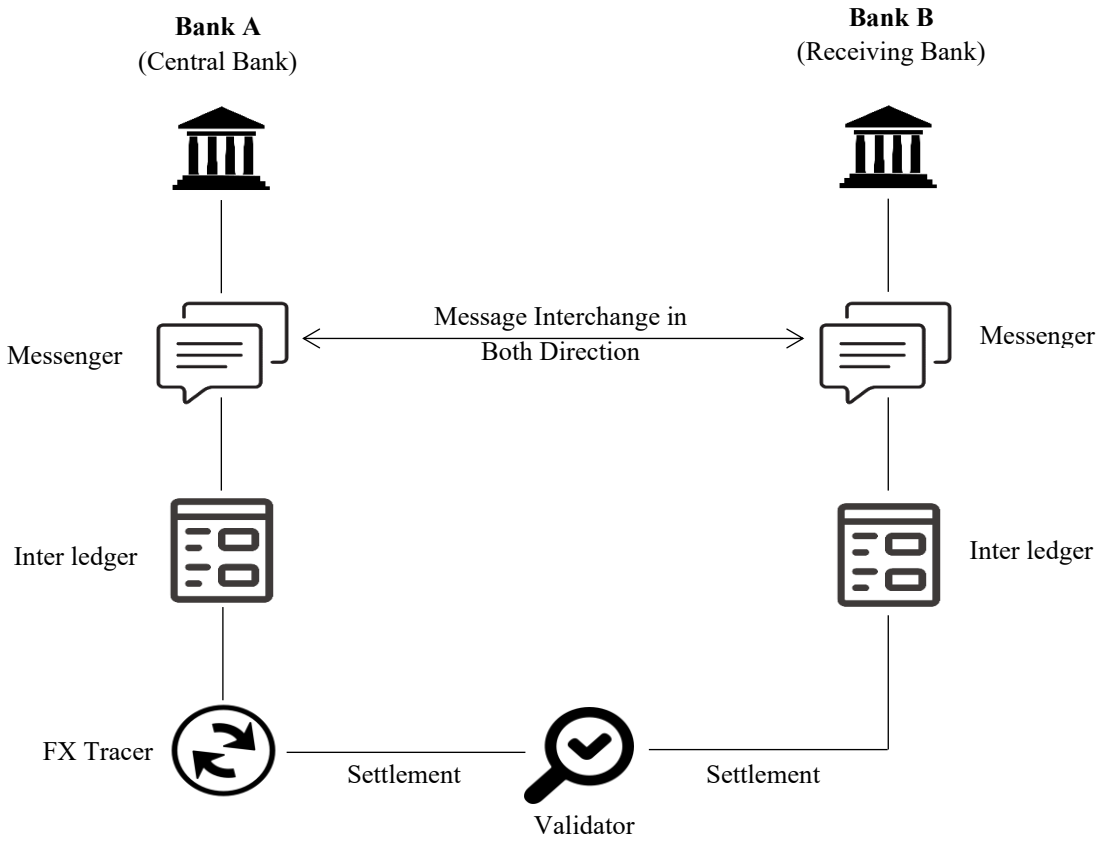

Fig. 3: Ripple Network Transaction Process Flow.

i) Messenger

Messenger establishes the connection between sender and receiver bank through Ripple network. Using this connection, both parties exchange the KYC, foreign exchange rate, charges, mode of payment, and expected time frame. After collecting this information, they send it to the originating bank as well as provide the total transactional cost. Before initiating the Transaction, the transacting party needs to check all the above-mentioned information. The sender then approves the Transaction, and the messenger sends the notification to all the related parties through ILP to settle the fund.

ii) Inter ledger

It is a sub-ledger that records general ledger information of the transacting bank. Inter ledger kept the track records of the transacting parties' debit, credit, and liquidity information. It also helps to do all the settlement processes automatically on a real-time basis. This feature is completely a new feature to the traditional SWIFT system.

iii) FX Ticker

It is one of the components of the Ripple network that provide an exchange rate between the sender and receiver ends' ledger and update accordingly. It also keeps the information of the transacting account, transacting currency, and authenticity of the ILP Ledger. When the sender bank makes the payment, the Fx Ticker sends the information to the ILP Ledger to conduct the settlement process, ensure the validity of the Fx quote and ensure the payment transfer process to the beneficiary's bank Inter ledger. The sender bank converts the local currency to XRP and this XRP cryptocurrency send to the receiver's bank through the Ripple network.

iv) Validator

Validator validates the Transaction cryptographically to the receiving bank whether the Transaction is a failure or a success. It also minimizes the additional settlement time and reduces the transactional cost as well.

With the consideration of technological advantages, transactional efficiency, operational cost, transaction time, and settlement time, more than 100 banks are worldwide are using the Ripple network [17]. On the other hand, SWIFT is a lengthy process that might take additional time to complete the entire process.

3.1 Implementation challenges of Ripple Network

Though Ripple has become a success to use the Ripple network for cross-border payment by using a cryptocurrency called XRP, there are still a significant number of challenges that need to address before going live across the globe. A few numbers of challenges are highlighted below:

i) Technology

Ripple is a used blockchain-based payment platform that is new for most users in the financial industry. The payment method supports its' cryptocurrency called XRP. Ripple uses a consensus mechanism and connects all the member banks in their network. It is entirely vendor-dependent, and technical experts are very rear, especially in financial institutes.

ii) Centralization

The 'Trusted vendor' concept is used to verify the Transaction in the Ripple network to maintain transactional integrity. Users are not entitled to get the incentive to validate the Transaction. So, fewer users are interested in validating the transactions, which leads to high-security risks.

iii) Pre-Mining

The pre-mining protocol is used to release a certain amount of XRP on a regular interval basis. Investors may think that Ripple may generate a huge amount of XRP, and the value of cryptocurrency may be fallen drastically.

iv) Legal Issue

All financial institutes are controlled, supervised, and monitored by the central bank of their respective country. Economic Affairs Committee forum is working on the central bank digital currency issue but not regulated yet. XRP is a cryptocurrency like other cryptocurrencies. Before initiating cross-border payment worldwide, the central bank needs to publish authorized policy guidelines for cryptocurrency or digital currency. To date, central bank policy is not available for XRP or any other cryptocurrency.

v)XRP volatility

XRP is a type of cryptocurrency like other cryptocurrencies. The price of this currency fluctuates like others,

so the investors are worried before investing the money in XRP. Properly addressing cybersecurity is another notable concern of this currency.

4. COMPARISON BETWEEN SWIFT AND RIPPLE NETWORK

Table 1: SWFT vs Ripple

Particulars	SWIFT	Ripple
Mode of operation	Exchange of data.	Exchange of value.
Transaction capability	SWIFT can handle up to 1,000 transactions per second.	Ripple network is capable of handling up to 1,500 transactions per second.
Members	More than 11,000 member institutions.	More than 100 member banks.
Intermediator	SWIFT works like an intermediator between sender and receiver institutes.	Intermediator is not required. The sender bank can pay directly to the beneficiary's bank account
Currency handle	All types of currencies are supported by SWIFT.	Support only own cryptocurrency called XRP.
Controlling authority	Controlled by regulators and central banks of the respective country.	Controlled by the vendor itself. Not controlled by central banks and regulators.
Consensus protocol	No consensus protocol is used in SWIFT	The consensus protocol is a mandatory requirement to initiate any transaction.
Platform size	biggest payment platform for Cross-border payment in the financial industry.	At the initial stage.
Payment settlement process	The payment settlement process is complicated and lengthy.	Ripple network supports the real-time payment settlement process.
Network Speed	Transaction completion time from sender to receiver is comparatively slow than Ripple network.	Due to the real-time nature of payment, the Transaction can complete within a few seconds.

5. CONCLUSION

The traditional method for cross-border payment SWIFT network is much slower than the blockchain-based Ripple network. The payment settlement process is a very complicated and high risks bearing system in SWIFT. On the other hand, the transaction and payment settlement process is completed together on a real-time basis. Though. SWIFT is the leader of the remittance market in financial sectors, especially for cross-border payments. Ripple will dominate the payment industry within a short period. Ripple networks support the cryptocurrency, distributed ledger, using cryptographic digital signature, and highly secure technological platform which supports pay directly from sender to beneficiary's bank account. But SWFIT does not support the distributed ledger and cryptocurrency which leads to slow the payment process. Transaction turns around time support 24X7 with low transactional cost in Ripple network. The Ripple network is developed based on the new technology that will bring a new dimension, especially for the cross-border payment in financial industries.

REFERENCES

[1] S. Seth, "How SWIFT Works?", https://www.investopedia.com/articles/personal-finance/050515/how-swift-system-works.asp. Updated on April 20, 2021.

[2] M. Reboucas, G. Pinto, F. Ebert, W. Torres, A. Serebrenik, and F. Castor, "An Emperical Study on the Usage of the SWIFT programming language", *2016 IEEE 23rd International Conference on Software Analysis, Evolution, and Reengineering (SANER); IEEE,* May 23, 2016.

[3] S. Zutautas, ToughNickel: "What is Telex Teletype Machine and How Does It Works", https://toughnickel.com/industries/Telex-Machine-What-It-Is-And-What-A-Telex-Operator-Does], June 28, 2021.

[4] S. Jani, "An Overview of Ripple Technology and Its Comparision with Bitcoin Technology", https://www.researchgate.net/publication/322436263, January 2018.

[5] Q. Deng, "Application Analysis of Blockchian Technology in Cross-border Payment," *Advances in Economics, Business and Management Research,* vol. *126,* 2020.
[6] J. Frankenfield, "What is Ripple?", https://www.investopedia.com/terms/r/ripple-cryptocurrency.asp, November 03, 2021.
[7] F. Armknecht, G.O. Carame, A. Mandal, F.Youssef, E. Zenner, "Ripple : Overview and Outlook", *International Conefernce on Traust and Trustworthworthy Computing, pp 163-180,* 2015.
[8] F. M. Benčić, and I. P. Žarko, "Distributed ledger technology: Blockchain compared to directed acyclic graph," *In 2018 IEEE 38th International Conference on Distributed Computing Systems (ICDCS) pp.1569-1570). IEEE,* 2018.
[9] A. Hammond. SWIFT gpi vs. Ripple? http://www.bobsguide.com/guide/news/2018/Feb/9/swift-gpi-vs-ripple-editors-picks. February 9, 2018.
[10] Business Identifier Code (BIC), SWIFT, https://www.swift.com/standards/data-standards/bic-business-identifier-code.
[11] S. Dasgupa, P. Grover, "Critically Evaluating SWIFT's Strategy as a Monopoly in the Fintech Business", *International Journal of Innovative Technology and Exploring Engineering (IJITEE), Volume-8, Issue-12,* October 2019.
[12] Invision Community, "Think You Know XRP?," www.xrpchat.com/topic/think-you-know-xrp/, November 2017.
[13] Ripple net, "The Financial Network of the Future", https://ripple.com/ripplenet.
[14] M.R. Islam, M.M. Rahman, M. Mahmud, M.A. Rahman, M.H. Mohamad, and A.H. Embong, "A Review on Blockchain Security Issues and Challenges", *2021 IEEE 12th Control and System Graduate Research Colloquium (ICSGRC), 2021, pp. 227-232, doi:10.1109/ICSGRC53186.2021.9515276.*
[15] S. Nakamoto, "Bitcoin: A peer-to-peer electronic cash system," Manubot, 2019.
[16] Z. Zahoor, et all., "Challenges in privacy and security in banking sector and related countermeasures," *International Journal of Computer Applications*, vol. *144*(3), pp. 24-35, 2016.
[17] Farmer, "Full List of Ripple Customer (2019/2020 Updated), https://www.publish0x.com/xrp-community/full-list-of-ripple-customers-20192020-update-xmjwkg, October 17, 2019.

ASIAN JOURNAL OF ELECTRICAL AND ELECTRONIC ENGINEERING
Vol. 2 No. 1 2022
E-ISSN: 2785-8189

Characteristic study for wireless Charging system

S. M. A. Motakabber, AHM Zahirul Alam, Nur Fadillah binti Jamal and Mazbahur Rahman Khan

Dept of ECE, Kul. of Eng., International Islamic University Malaysia (IIUM), Jalan Gombak, 53100 Kuala Lumpur, Malaysia

*Corresponding author: amotakabber@iium.edu.my

(Received:28th January 2022; Accepted: 1st April 2022)

Abstract—Power is an essential requirement in these modern lifestyles. Electronic gadgets like cell phones, laptops, etc., need the least power to charge. The utilization of Wireless Power Transmission (WPT) has been a hot issue among researchers these days. Nowadays, the application of wiring is becoming very inconvenient since everything cannot be used as there are some limitations and dangers. Therefore, several techniques have been found to carry out the wireless charging purpose in this study. The power transmission through the air is much easier to implement, more efficiently and persistently charged without the demand of connection physically. In this paper, a comparison between the three techniques for wireless power chargers has been determined. Among these three, it is found that the utilization of inductive coupling techniques is the best way to implement the system.

Keywords: *Wireless Power Transfer, Wireless charging, WPT*

1. INTRODUCTION

Recently, power has been a significant source in our everyday life. The usage of power that is required in every device like a phone, laptop, and other electronic gadgets has to be powered every minute. An individual is vigorously reliant on gadgets because of different intentions, including correspondence, web surfing, and enjoyment. These gadgets are reliant on batteries for their activity. The motivation behind these batteries is to store vitality and convert that putaway vitality into an electrical frame at whatever point is required. These days, the necessity of wiring installation has been very hassle, dangerous and sometimes impossible.

Wireless power transfer is beneficial and popular among the urban generation with flexibility, especially for gadgets that need frequent changing of batteries or needs cables for charging purposes. However, it is not practical to consistently acquire a plug point or even maintain the charger with oneself. Latterly, the evolution of the cordless charging mechanism is considered a transformation technology in the mobile world with the aid of many massive smartphone manufacturers involving Samsung and Apple.

There is a large market interested in this field as it is an easy, inexpensive and standardized resolution for consistently empowered devices. Therefore, it is helpful to classify these sciences in terms of their fundamental power exchange component to comprehend the significance of a range, adjustment, and effectiveness.

2. WIRELESS CHARGING TECHNOLOGIES

The consequence of wireless technology has been rooted in Nikola Tesla, who demonstrated lighting 200 bulbs apart 40km away through wireless power transmission [1]. A coil called resonant transformation or tesla coil has been formed, but its electrical field was dispersed. Although the experiment had little success, wireless power transfer was the most researched area in his time. Presently, electronic gadgets have been increasing as it uses batteries for their work. Without a battery, all these gadgets cannot be used since the heart requires frequent charging. A rectifier, filter, and cable of a certain length are the main component of ordinary charging which indirectly reduces the portability of the gadgets during the charging. Today, there are already implementations of wireless charging around the world. Fig. 1 illustrates a typical wireless power transfer system (WPTS).

The transmitter is fed by the input power and converted from AC to DC by rectification. Next, the DC voltage is converted back into AC with variable frequency. A high frequency is used in the transformer to increase the magnetic fields. The high frequency is delegated to the transmitter coil via a certain circuit based on the block

diagram above. At a certain frequency level, the receiver coil receives this transmitted power. From here, the load is not directly be fed. After rectifying, the power is disposed to a voltage regulator that manages the voltage to avoid damage to the load. A connection between the receiver output and transmitter input is rooted in the needed level of power transmitted to the load. The transmission should be stopped via the controller, and else ways extreme supply of power will harm or affect the load.

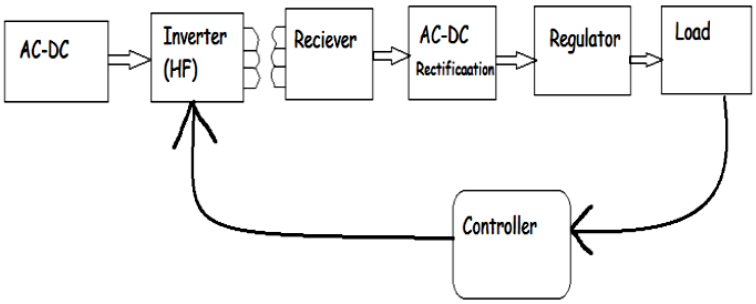

Fig. 1: Flow diagram for WPT [2]

Wireless technology generally can be divided into three techniques: magnetic inductive coupling that the most used; magnetic resonance coupling, which is moderately used; and non-directive RF radiation, which is relatively new in this area [2]. Radically, the magnetic inductive and magnetic resonance coupling acted on a short distance range where the propagated electromagnetic fields lead to the area near the transmitter or circulation object. The near-field power is dissipated based on the cube of the reciprocal of the charging length. In another way, microwave radiation should be used for the far-field because of the distance range. According to the square of the reciprocal charging length, the far field power will decline as the range of distance increases.

Additionally, the radiation penetration does not impact the transmitter using the far-field technique. Yet, the penetration of radiation affects the load on the transmitter. The reason is that the antenna of the transmitter and receivers are not coupled when using the far-field technique. Meanwhile, the transmitting and receiving coils are coupled for the near field [2].

2.1 Inductive coupling

Inductive coupling is when the magnetic field induction delivers the electrical energy between two coils. For example, inductive power transfer (IPT) produced during a primary transmitter's primary coil propagates a broadly changing magnetic field across the secondary coil of the receiver inward the field that is shorter than a wavelength. As shown in Fig. 3, the short distance magnetic power induces the voltage/current via the secondary coil of the receiver inward the field [2]. The secondary coil must be integrated at the operating frequency.

Many scholars have used this technique for research purposes. Many of them successfully use this technique to provide wireless charging for gadgets. According to a research paper [3], they proposed to charge a laptop that produces a voltage of 19.5V at 2.3A, using a single-ended primary inductor converter at the receiver to buck-boost the voltage and PI controller for controlling the output for variation in the distance within the transmitter and receiver coils. Respectively, the output gain is 20.7V at 2.5A [3].

Another study introduced a cognitive wireless charger (CWC) that can cope with the operating frequency in real-time using implicit response from detecting for optimal operation [4]. Subsequently, when the CWC is switched off, their prototype has a commensurable function to the Qi wireless charger. When the CWC is switched on, the prototype indicates a powerful improvement over modern wireless charging [4]. A self-alteration power transfer location wireless charging system has been proposed and demonstrated related functionalities of the desired wireless charging via the Bluetooth Low Energy (BLE) Module [5].

There are some favours of magnetic inductive coupling, including the easiness of implementation, adaptable operation, excellent performance at close distance and security. Thus, it is the most frequent technique used primarily for mobile gadgets.

2.2 Magnetic Resonance Coupling

Based on Fig. 3 above, an illustration of a working system for magnetic resonance coupling is shown as the electrical energy between two resonance coils by changing or oscillating magnetic fields generated and transferred by evanescent wave coupling [2]. Surprisingly, it is reported that MagMIMO had distinguished and cast greater

energy for a phone even it is put inside the pocket. More presently, an innovation of wireless charging technology published by Massachusetts Institute of Technology (MIT) Scientist which successfully charged wireless gadgets maximize up to 30cm.

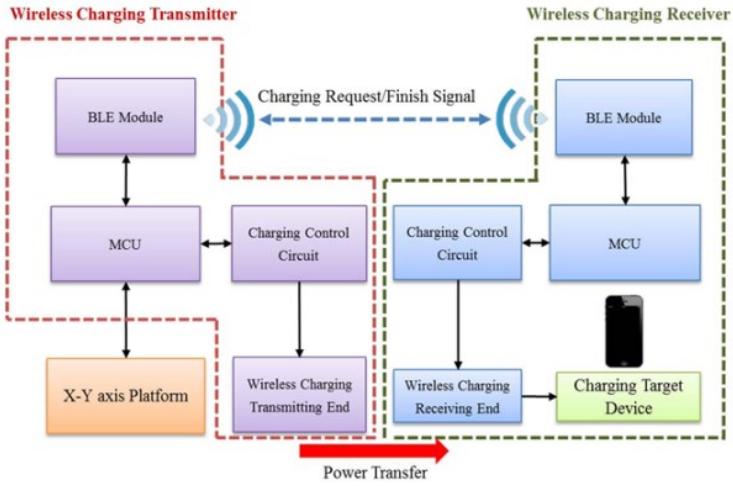

Fig. 2: BLE Module for WPT [5]

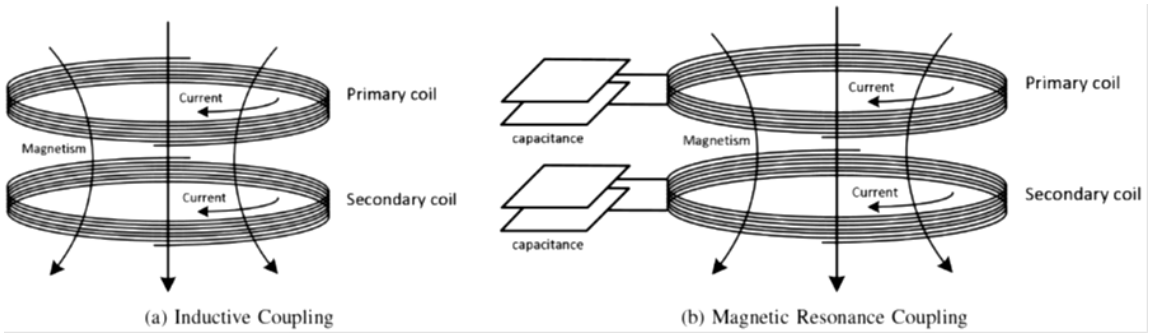

Fig. 3: Inductive coupling (a) and magnetic resonance coupling (b)

Besides this, another successful finding is the ability to charge a phone with more than 3W in a range of 5 to 15cm with varying angles, which are using a resonance frequency of 6MHz [6]. Moreover, the distance range between transmitter and receiver (phone) can maximize up to 20 cm for lower charging. It is beneficial to use this technique as it is simple, low-cost and provides a large area for both wireless charging, either handheld or on-table charging. A paper uses a microstrip to implement a radiator for transmitting and receiving at a frequency of 10MHz AC signals that detach each other in minimal space to gain the optimum coupling. As a result, the researcher demonstrates a 0.8mm distance of radiator the wireless power charging system with the capacity to supply 4.08V DC as the output of the receiver circuit that charges a phone battery. In contrast, the voltage at the transmitter circuit is equal to a 12Vpp AC signal.

It is found that implementing a repeater coil that is located at the transmitter active coil at the identical plane as the transmitter coil beyond a direct feeding can accommodate more power transfer efficiency, which is more than 10%, with a maximum spacing distance of about 300mm. Regarding this paper [7], the authors discover source-to-load inductive connection under resonance restriction for power transmission through contactless. They use two different load quantities: one load-loop and two load-loop. Magnetic reflected impedance plots with changing load and frequency restriction show a progression under resonance frequency identical to the power source [7].

One more study presented [8] a result with a maximum distance of 1.21m with a full design system consisting of a function generator, Class B power amplifier, transmitter helical coil, and rectangular planar receiver. The difference is that they are using transmitter and receiver similar to each other in terms of sizing and shape [8].

2.3 RF Radiation

RF radiation is defined as a diffusion of RF/microwave as an intermediate to carry beaming energy that is applied by the RF radiation. RF/microwave increases over the space at the speed of light, basically in line-of-sight with a common frequency range between 300MHz and 300GHz [2]. Therefore, the structure of the microwaves power transmission system is built for a far-field wireless charging system. In the latest research in a paper [9], researchers are using the Wi-charging approach that utilizes a laser as an optical source to charge wireless devices, but, unfortunately, this concept has a poor coverage zone and only works in indoor bounds.

Achmad Munir also agrees with this in his paper [10], which successfully gained an average efficiency of around 58% and a high frequency of 10MHz when the division between 2 stacked radiators is 0.8mm, where the radiator is constructed using the spiral shape of microstrip patch. Furthermore, an antiparallel resonant loop was designed in a paper. A reduction of magnetic field effectiveness of almost 6dB is gained and differentiated to a conventional loop at a calculated length maximum of 10m. Thus, a good improvement is achieved when using this technique with a variety of methods.

In conclusion, the best method to use is using Magnetic Resonance Coupling. It is because the optimal charge can be achieved as the system's architecture is not too complicated. Besides, it also has the advantage of being used at a range of distance far more than Magnetic Inductance Coupling, which is far field. The difference between these two techniques is electrical energy gained by the resonance coupling through a varying or oscillating magnetic field. Regarding the RF/microwave radiation, this technique was not yet well-known by many people as the efficiency was low because of the line of sight. Thus, radiation is not suitable for choosing as a good technique for wireless charging systems for gadgets.

3. ALGORITHMS FOR WIRELESS POWER TRANSFER

The theory of inductive coupling for wireless power transfer was based on Maxwell's equation. First, magnetic flux was produced by the current going through a conductor. Then the electric field is created by different magnetic fields. Thus, this electric field will accelerate the electric charge, and the current will produce. The circuit's geometrical shape, conductor structure, and permeability of the medium will define the inductor coil. Furthermore, the inductor of two coils is controlled by the range and relative structure of these coils. The coupling coefficient is defined as:

$$k = \frac{M}{\sqrt{L1\ L2}} \qquad 0 \leq k \leq 1 \tag{1}$$

This coefficient calculates the magnetic coupling of these coils and is self-reliant on the number of turns in these two coils. The phase shifts can be created because of these two elements, which are inductances and capacitances. The impedance equation determines the phase shift.

$$Z_l = j\omega L \tag{2}$$

$$Z_C = \frac{1}{j\omega C} \tag{3}$$

In the engineering and physics world, the Quality factor (Q-factor) is determined by a greatness parameter that defines an oscillator's aspect or another named a resonator. Q-factor is said to be higher if the greater amplitude. For an ideal circuit of RLC, Q-factor is defined as:

$$Q = \frac{1}{R}\sqrt{\frac{L}{C}} \tag{4}$$

Where R is resistance, L is inductance, and C is capacitance, respectively. For a single layer inductance (air-core), Wheeler's formula is used to calculate the value of inductance as the formula:

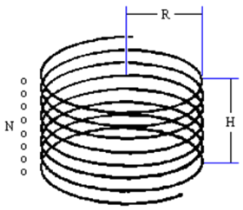

Fig. 4: Illustration of the coil

$$L = \frac{N^2R^2}{2.54(9R+10H)} \quad (5)$$

Were,

L = inductance (micro-Henry)
N = number of turns of copper wire
R = radius of the coil (cm)
H = height of the coil (cm)

4. SIMULATION USING PSPICE

In this project, a rough simulation of the circuit is conducted. Following is the schematic circuit of the simulation using PSPICE. During this process, simulations between inductance and resonance are conducted. RF radiation technique was not conducted as it needs a proper line of sight propagation. The inductance schematic circuit is shown in Fig 5.

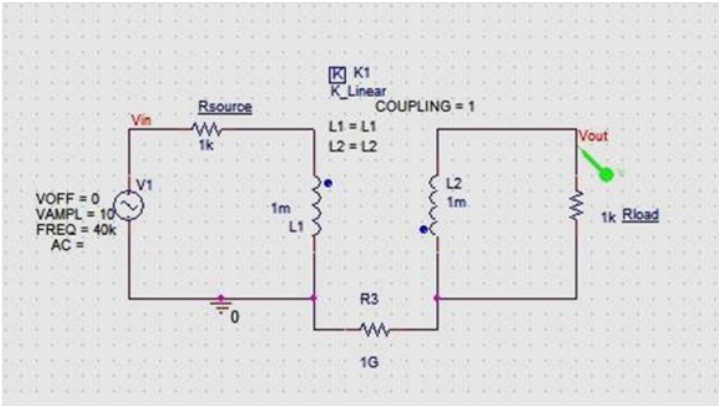

Fig. 5: Schematic diagram for Inductive Coupling circuit

Next, magnetic resonance coupling simulation was taken care of with different positions of capacitance was constructed to determine the variation of the data taken. The figures above show that 1G Ohm of resistance was structured. It is due to the simulation environment presenting reference and DC track to entire nodes. If the resistance is not implemented, the simulation will notice an error in the floating point. This resistance will effectively provide secondary inductance floating and give a DC track and a ground remark for the whole simulation.

The results of these simulations are included in section V. Here, the air gap separates the transmission unit and receiver unit to get complete power transfer without any obstacles.

5. RESULT EXPERIMENTAL

Fig. 6 shows the complete experimental setup used to verify the theoretical model based on the simulation result in the PSPICE. The transmitter part consists of an NPN3055 transistor and a 1kΩ resistor. The transistor is connected to the function generator to generate frequency accordingly. This transmission part is associated with the primary coil linked with the DC power supply of 9V. The enameled-copper wire produces magnetic propagation between the transmitter and receiver. The diameter of the enameled-copper wire used is 0.06mm. It was built with the air-core inside. The copper wire is winded side by side without overlap in 10cm diameter of cardboard. The part consists of a resistor of 10kΩ and 0.01µF of the capacitor at the receiver. This resistor and capacitor are connected in parallel along with the secondary coil. It can be seen that the transmitter and the receiver are not connected. They communicate with each other only in the wireless medium. The simulation result shows that magnetic is a better choice than inductive coupling. The power increases as the frequency also increase. Even though the outcome seems similar, if we change the parameter of the simulation, there will be slight differences in data corresponding to the frequency used, the number of turns, and the value of the capacitor. The prototype was built based on the simulation circuit of the inductive coupling method but using different values. Fig. 6 shows the complete setup of the prototype.

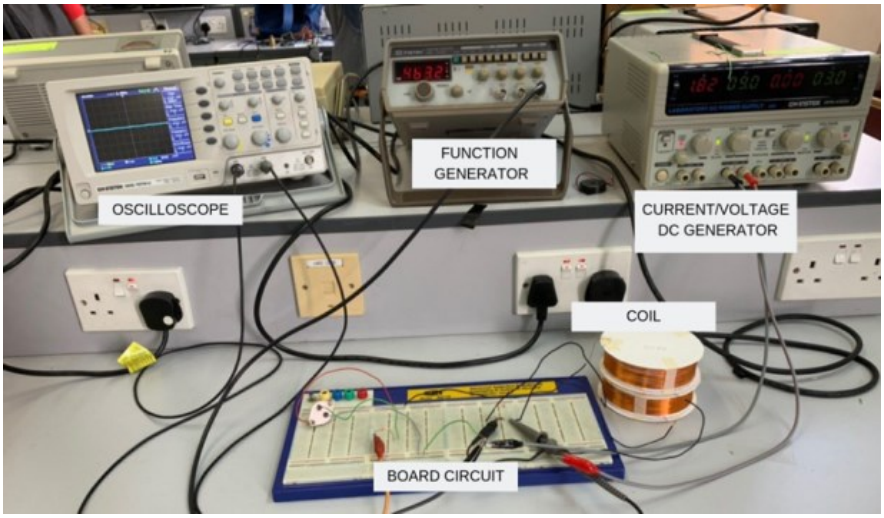

Fig. 6: Full setup of the prototype

The result of the project was taken first with a variation of frequency with the distance of zero between two coils. Then, the number of turns differs as a pair of 10 turns was created, also for 20 turns and 30 turns. The diameter of the coil is 10cm. The coil was set up and down, as shown in the figure, and the value of Voltage peak-peak was taken. The design parameters and inductance value are shown in Table 1.

Table 1: Parameters values

Coil	Resistor (kilo-Ohm)	Capacitor (micro-Farad)
Transmitter	1	-
Receiver	10	0.01

After the optimum value was reached, the voltage rapidly decreased with higher frequency. It is observed that 10 turns of coil need a higher frequency than 20 and 30 turns of coil to reach its optimum value. Besides that, the voltage value for 10 turns is less than the other two coils. However, it is slightly different for the 20 and 30 turns. Therefore, the optimum voltage value is almost the same with different frequencies. Next, the power received from the measured value of voltage is calculated by using the formula as follows:

$$P = \frac{V^2}{R} \tag{6}$$

Fig. 7 shows the power received at the receiver part according to the number of turns. As seen in the figure, the value of the power is at the highest when the value of the coil is 30, equal to 0.621W. When the number of turns is 20, the power is equal to 0.596 W and at 10 turns equal to 0.110W. It is proved that the power is directly proportional to the voltage. At a certain point, when it reaches the optimum value, the power value decreases with a higher frequency. This is because of the resonant frequency where the system oscillates with larger amplitude at several frequencies.

The experiment is varied with different capacitor values at the receiver part with 1.5nF Farad. Voltage peak-to-peak of 10, 20 and 30 turns are measured accordingly. Thus, the result of the power is calculated. As shown below are the result of the experiment. The power value of this experiment can be seen as a bit of bit low than the previous value of the capacitor. In this experiment, the maximum power that can be reached for 30 turns is equal to 0.292W, followed by 0.141W for 20 turns and 0.017W for 10 turns of the coil. The value of power decreases with the decreasing value of the capacitor. Thus, in other words, the power received depends on the value of the capacitor.

To determine the efficiency of the power received from this project is by changing the distance between the transmitter coil and the receiver coil. By separating these two coils (air gap), the ability to transfer power between the transmitter unit and receiver unit can be calculated. This experiment is conducted based on the optimum frequency value from the previous experiment. As the value of voltage decreases by the value of distance, only a few data can be collected for n =10. The value of L for n =10 is 1cm, 2cm for n = 20 and 3cm for n = 30.

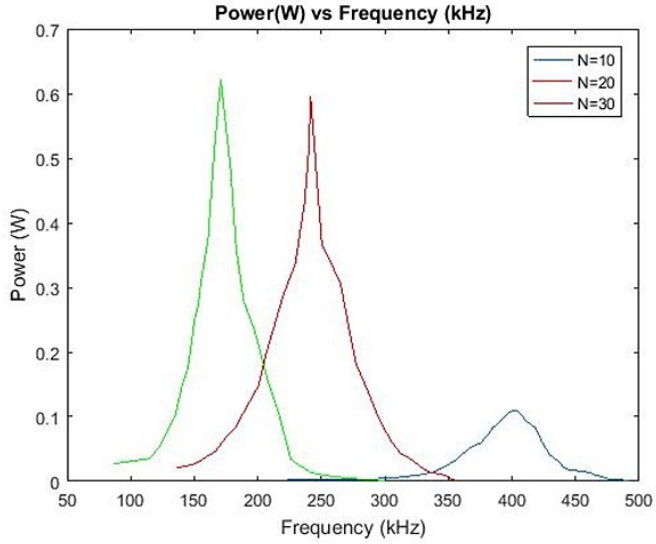

Fig. 7: Power versus frequency with different values of n

Here, the most challenging part of experimenting with is to fix the coil of the receiver part placed at a parallel distance. To get the value, we place a giant plate at the top of the coil and the ground so that we can vary by putting an object side by side near the coils. Based on the figures, 30 turns of a coil can transfer up to 2.304mW at a 13cm air gap. Therefore, power transfer for this experiment is horrible because of the only small amount of power that can be transferred. Therefore, the best solution for this inductive coupling is to put the transmit unit and receiver unit very close to each other to have a more efficient power transfer.

6. CONCLUSION

In conclusion, this project will bring future advancements in wireless power transfer technology for electronic gadgets. By using inductance and magnetic resonance coupling, wireless power transfer has their specialization according to the method used. The optimum value using inductance coupling had been measured and calculated. The inductance coupling method can achieve up to 0.621W in zero distance between the transmitter and receiver. However, the ability to transfer the power with an air gap is up to 13cm, and the power is only 2.304mW. Thus, it is not suitable for wireless power transfer along with distance.

The verification and simulation technique has been done for inductance and magnetic resonance coupling. However, only inductance coupling data is determined using an experimental hardware test.

REFERENCES

[1] G. Bekaroo and A. Seeam, “Improving wireless charging energy efficiency of mobile phones: Analysis of key practices,” 2016 IEEE Int. Conf. Emerg. Technol. Innov. Bus. Pract. Transform. Soc. EmergiTech 2016, pp. 357–360, 2016.

[2] X. Lu, D. Niyato, D. I. Kim, and Z. Han, “Wireless Charging Technologies: Fundamentals, Standards, and Network Applications,” IEEE Commun. Surv. Tutor., vol. 18(2), pp. 1413–1452, 2016.

[3] P. A. Asokan and I. Mamatha, “A novel approach to wireless power transfer,” Proc. 2017 IEEE Int. Conf. Technol. Adv. Power Energy Explor. Energy Solut. an Intell. Power Grid, TAP Energy 2017, pp. 1–6, 2018.

[4] S. Y. Chang, S. L. S. Kumar, and Y. C. Hu, “Cognitive Wireless Charger: Sensing-Based Real-Time Frequency Control for Near-Field Wireless Charging,” Proc. - Int. Conf. Distrib. Comput. Syst., pp. 2302–2307, 2017.

[5] Y. H. Zhang et al., “An implementation of an automatic adjustment power transfer position wireless battery charging system for mobile devices,” 2017 IEEE 6th Glob. Conf. Consum. Electron. GCCE 2017, vol. 2017–Janua, no. Gcce, pp. 1–2, 2017.

[6] I. Yasar, L. Shi, K. H. Bai, X. Rong, Y. Liu, and X. Wang, "Mobile phone mid-range wireless charger development via coupled magnetic resonance," 2016 IEEE Transp. Electrif. Conf. Expo, ITEC 2016, 2016.

[7] K. J. Ahmed, N. I. Zainal, S. Hafiz, R. Mizan, S. Khan, and A. N. B. Nordin, "Wireless Power Transmission - Exploring source to load inductive link under resonance and varying load condition," Proc. - 14th IEEE Student Conf. Res. Dev. Adv. Technol. Humanit. SCOReD 2016, pp. 4–8, 2017.

[8] M. Abdou, "Wireless Power T Transmission Enhancem ment Using etic Resonance Couplin Magne ng," Int. Conf. Signal Process. Commun. Power Embed. Syst., pp. 1329–1331, 2016.

[9] C. Pani, O. Ray, A. Ghosh, Z. Qadir, M. M. Sarkar, and W. Reja, "Wireless power transfer using free space photonics," Proc. - 2016 Int. Conf. Adv. Comput. Commun. Autom. (Fall), ICACCA 2016, 2016.

[10] A. Munir, N. W. Dessy Eka Rahayu, and B. T. Ranum, "Radiator of wireless power charging for mobile device and its efficiency characterization," INTELEC, Int. Telecommun. Energy Conf., vol. 2016–Septe, no. 1, pp. 2–5, 2016.

ASIAN JOURNAL OF ELECTRICAL AND ELECTRONIC ENGINEERING
Vol. 2 No. 1 2022
E-ISSN: 2785-8189

GPS and GSM Based Vehicle Tracker

S. M. A. Motakabber, AHM Zahirul Alam, Mohamed Reda Maurice Francis and Syed Ahmad Fawwaz Wafa

Dept of ECE, Kul. of Eng., International Islamic University Malaysia (IIUM), Jalan Gombak, 53100 Kuala Lumpur, Malaysia

*Corresponding author: amotakabber@iium.edu.my

(Received:28th January 2022; Accepted: 1st April 2022)

Abstract—Nowadays, electronic wireless vehicle tracking is becoming essential for preventing car theft and emergency services in vehicle accidents. There are three types of vehicle tracking systems in the market. Each has its advantages and disadvantages. Based on the working principle, these trackers are classified as cellular phone-based trackers, wireless passive trackers, and real-time satellite trackers. This paper has discussed designing and developing a vehicle tracking system using an Arduino microcontroller, GSM, and GPS modules. The proposed design is a different approach to these vehicle tracking systems. The function of the tracker is done in three steps; first, it connects the hardware components and tests the connectivity; when the secure connectivity is confirmed, it executes the write command for the connected GSM and GPS modules. Finally, it tracks the target vehicle, collects the GPS coordinates, and processes the data using the software. The proposed design has been verified by MATLAB simulation, and the results obtained are satisfactory for both simulation and practical examination.

Keywords: *GPS, GSM, Tracker, Vehicle tracking, RFID, Arduino microcontroller*

1. INTRODUCTION

The GSM (Global System for Mobile Communications) is a level made by the European Telecommunications Standards Institute (ETSI) to classify the protocols for second-generation (2G) digital communication designed for cell phones, which prevailed in Finland in July 1992. As of 2014, it has become the practical worldwide standard for mobile networks.

However, the GPS (Global Positioning System) is a global navigation satellite system that supports the location and time information to a GPS receiver anywhere on or close to the globe. There is an unblocked vision of four or more GPS satellites. The GPS works freely on any phone or internet receiving, although those technologies can increase the GPS positioning information's advantage. GPS supports many critical locating abilities for the army, social, and trading consumers worldwide. The US government designed the system, controls it, and allows it to be independently attainable to anyone with a GPS receiver. However, the United States government can suitably decline entry into the system. Integrating both technologies can produce high capabilities and usefulness for positioning, communication, and safety.

2. TRACKING SYSTEM WITH SENSORS

Rathinakumar and Manivannan (2012) proposed three modules for the car tracking system, automatic velocity monitor system, detecting accidents module and protection access module, as shown in Fig. 1. A control module, an RF transmitter (Tx) and an RF receiver (Rx) are used to monitor spontaneous speed. The contactless sender can transmit the information up to 30 meters away from the car. The RF module used a free spectrum carrier frequency of 418 MHz. The RF sender is placed in a suitable location, and the RF receiver is put in the car. When the vehicle attains a zone like a school or U-turn, it spontaneously decreases the velocity. When it reaches out of the location, it will spontaneously recover its velocity. Based on this, an accident probability is going to be decreased. The data transmitting modules, GSM, GPS, and various sensors have been implemented in the car. If accidents happen, the vibration sensor tests the vibration level. Suppose it overrides the threshold boundary. The module tries to find a chance of an accident at a specific location. The GPS detects the car position and transmits the data through the GSM module to the base station.

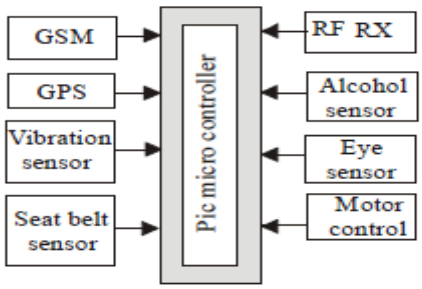

Fig. 1: Block diagram for the vehicle tracking system [1]

Nowadays, vehicle stealing cases are more significant than ever before to secure vehicle-efficient security with the only credible anti-stealing gadget. The vehicle protection gadget offers efficient security to the car. A vehicle with an electronic control unit protection system can help the owner immediately shut off doors when pressing a button. The main types of electronic control units (ECU) are manual or automatic. These systems could not give the absolute protection and attainability of the car in case of stealing. Thus, an improved system potentially uses a firmed system based on GSM technology [2].

2.1. Controller Area Network

In 2014 Prakash and Sirisha proposed an improved system with a monitoring system inside the car. This project aims to introduce a mobile connection to the firmed system. The automotive industry employs CAN (Controller Area Network) in-car network for engine management, body electronics such as door and roof monitor, air condition and light, for fun monitoring. Many car manufacturers have also started to design CAN-based car automation. CAN communications are employed in engine management to connect various ECUs. The vehicle manufacturing industry put a basic level of the protection system, like a warning system. SMS is an excellent method of connecting the traditional alarm because it is achievable and not expensive.

The scheme's concept is to adjust the various quality of the existing protection system, which will alarm the car's driver by transmitting SMS. When an invasion upon the car gives the resolution to stop car stealing in the cheaper than sophisticated protection vehicle system.[3].

2.1.1. A tracking system with RFID

In this proposed system, an RFID reader will be installed beneath the car to follow the landmarks of locations to known places like schools, hospitals, petrol stations, temples, etc. Every road will be connected with RFID tags. These RFID tags will include the data, such as the names of the locations around it. The presented burglary control system regains a geographical place and supplies a means to monitor the car's additional motion. The system is designed to make a trait that would control the vehicle's speed by (motor switching on/off) just onto reception of an established program in advance of the user, who may be at a distance through mobile phones.

Arduino is a low-cost microcontroller that uses simple interfacing, IoT [4] and many applications. A tracking system was proposed in [5] that included an Arduino to help make the process quicker. Once the vibration sensor gets the vibration measures the vibration from the accident's friction, the Arduino will send an SMS message containing the location through a GSM module; the location is obtained from GPS.

The concept of this design is to send data of the accident to the emergency car and relatives. GSM module is chosen to send the data by sending SMS messages and GPS technology to locate the vehicle. We use a GSM modem that has a SIM card. GPS location is included in the SMS sent to the ambulance to have precise information about the accident's place and time. Thus, a GPS module is used to elicit the accident place, and the GPS info should include the latitude, longitude, and altitude values. To function the GPS and GSM modules, an Arduino UNO board is used that contains a microcontroller. Arduino is an easy-to-use gadget that can be connected with some small sensors or modules. It is clear that the Arduino will transmit the SMS message by the GSM module by placing the GPS in the message gained from the GPS module. A vibration sensor is used to detect an accident and it is located in the vehicle. The vibration sensor is in the vehicle to perceive the vehicle's vibrations. When the driver collides, the vehicle strikes the land. The vibration sensor examines the vibrations resulting from the hit, and then the Arduino will transmit a message comprising data of the accident and its place. The Arduino microcontroller sends a short message to the mobile phone via a GSM module along with the facts that by accident

occurred and the exact position from the GPS module. The utilization of automobiles is on the rise as a great deal as injuries occur. The venture's overall characteristic is to detect the coincidence of the usage of the GSM and GPS modules interfaced with the Arduino controller. When the vehicle is subjected to an accident, the vibration sensor senses the amount of the vibration. When the amplitude is extra than the fixed restrict, the program is being triggered. The controller, instead of cutting-edge vicinity using GPS and switch that place the use of GSM to the emergency variety designated within the program and the coincidence car identity number.

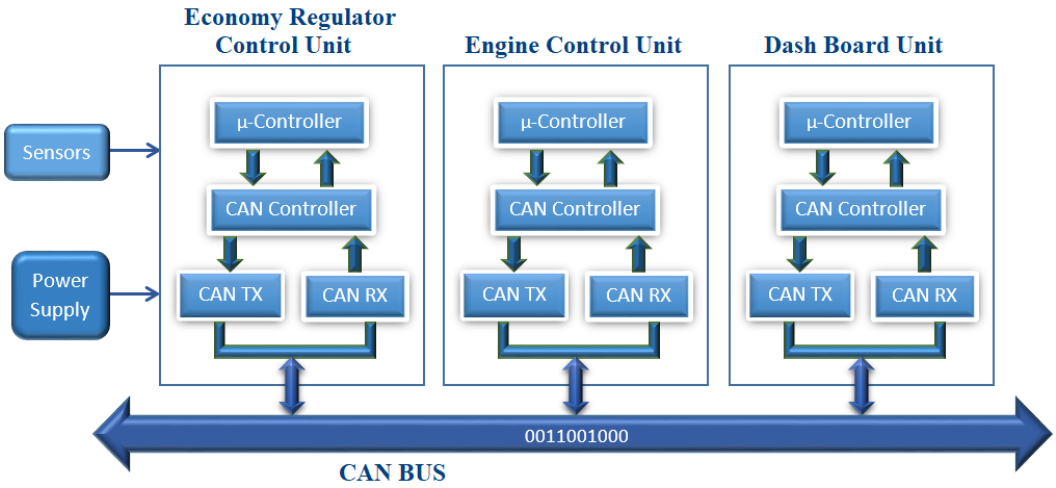

Fig. 2 Modified block diagram for the vehicle tracking system [3]

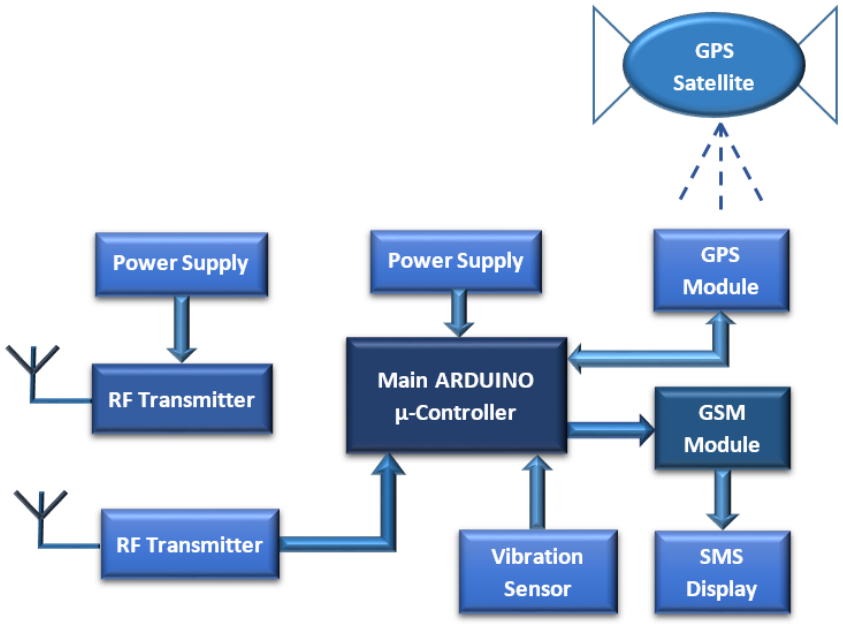

Fig. 3: Block diagram for the Arduino based system

3. DESIGN OF GPS GSM BASED VEHICLE TRACKER

MB102 Solderless Mini Breadboard: It has 400 holes, and its size is 8.5cm X 5.5 cm. The breadboard lets the user put on and off parts, and thus if there will be alterations or the user wants to make a quick circuit, it will be much faster than soldering up the circuit. Many breadboards that share the same size can be joined horizontal or vertical parallel. Breadboards are environmentally friendly. Jumper wires are an essential part that connects two or more devices. They come in many colours to be picked up the right one when many are on the breadboard.

Battery or power bank: to charge the whole system

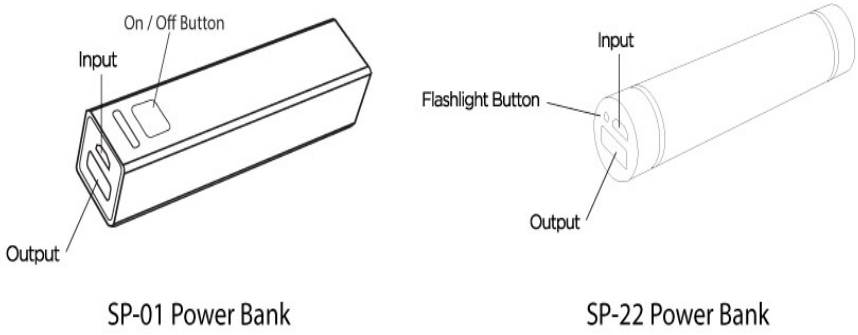

Fig. 4: Examples of power banks

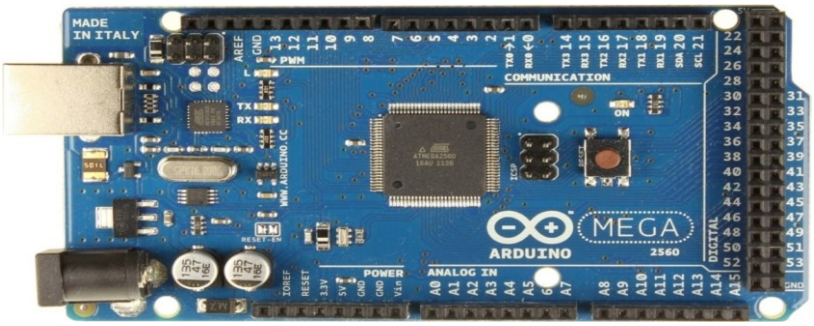

Fig. 5: Arduino MEGA 2560

3.1 SIM900A GSM GPRS Wireless Extension Module Board

The SIM900A is an inexpensive and easy Arduino GSM and GPRS module. It is available in the markets. The SIM900A is a complete Dual-band GSM/GPRS module in an SMT system that could be rooted in the user process, enabling gains from tiny dimensions and ineffective gains. It features an industry-standard interface, and the SIM900A delivers GSM/GPRS 900/1800MHz performance for voice, SMS, Data, and Fax in a small form factor and with little power consumption. With a small configuration of 24mm x 24mm x 3 mm, SIM900A can fit almost all the applications' space requirements

Fig. 6: SIM900A GSM GPRS Wireless Extension Module Board

3.2 GY-NEO6MV2 GPS Tracking Module with Antenna MWC AMP2.5

It comprises a ceramic antenna; EEPROM power-off data save; info saving battery; LED signal indicator lamp. Antenna size: 25 x 25mm; Module size: 25 x 35mm; Install hole dia.: 3mm; Default baud rate: 9600; Compatible with different flight controller modules NEO6MV2 GPS module has 4 plugs: Rx, Tx, Vcc, and GND, and that is simple to integrate with using Software Serial on a serial interface on an Arduino Mega. There is only one little problem: The module uses 3v3 logic, which is incompatible with Arduino's 5v. However, a simple voltage divider can solve this issue.

Fig. 7: GY-NEO6MV2 GPS Tracking Module

There is more than a manner to connect a GSM module to an Arduino. The connection between Arduino and GSM module is serial in style. Therefore, it's miles supposedly the use of serial pins of Arduino (Rx and Tx). Thus, if the device is used, connect the GSM module's Tx pin to the Rx pin of Arduino and the Rx pin of the GSM module to the Tx pin of Arduino.

An SMS message is to be despatched to the device, and it sends lower back the modern-day GPS vicinity inside the shape of an SMS. The GPS location is a Google Map hyperlink. The device constantly updates the GPS place to the most effective quantity unique within the code.

The Arduino MEGA controls the complete process with a GPS Receiver and GSM module on this undertaking. GPS Receiver is used to detect the car coordinates, and a GSM module is used to send the coordinates to the user via SMS.

The GSM module receives a despatched message linked to the system and sends the info to the Arduino MEGA. Arduino MEGA reads it and extracts the main message from the whole message, then compares it with the predefined message inside the Arduino MEGA. Arduino reads coordinates by extracting GPS info and sending it to the consumer through the GSM module if any fit takes place. The message consists of the coordinates of an automobile place.

Communication technologies developments have long considered passed the best functionality to get admission to others while shifting. Today, cell conversation devices are getting a whole lot extra sophisticated and offer extra than the capability to preserve communication. Smartphone GPS tracking is one of those advances.

All smartphones frequently ship a radio sign, despite the fact that no calls are occurring. As an end result, cellphone organizations were capable of predicting a smartphone's location for decades with the use of triangulation facts from the towers receiving the sign. However, introducing the GPS era into smartphones has intended that phone GPS monitoring now makes these records lots more correct.

The era of finding an area is based totally on measuring electricity stages and antenna styles. It uses the idea that a smartphone always communicates wirelessly with one of the nearest base stations, so it's far recognized which base station's smartphone is speaking. It is also known to be close to the respective base station.

Real-time monitoring is also useful from a safety viewpoint because it shall we car owners to specify the car's particular area at any time. In addition, the vehicle's GPS tracking system may be a useful resource for police training sessions wherein the automobile is taken to if it's far stolen.

The GPS module used on this assignment is GY-GPS6MV2 and wishes an electricity supply of 3V to 5V. It has a ceramic antenna and a sturdy signal connection. The EEPROM saves the configuration parameter records whilst the strength is down. It comes with a statistics backup battery. The LED signal lighting whilst running; it's

miles a visible way to see the module captures data. It has a default baud rate of 9600. It is well-matched with various flight manage modules and relatively small in length with a small antenna.

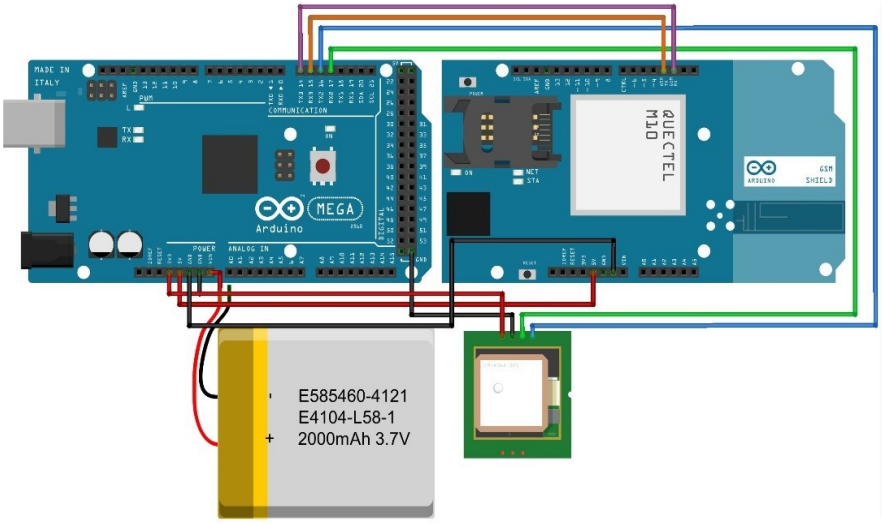

Fig.8: Proposed tracking module

SIM900A modem is made with twin-band GSM/GPRS primarily based SIM900A modem from SIMCOM. It operates on frequencies 900/ 1800 MHz. SIM900A can seek these bands mechanically. AT Commands can also set the frequency bands. The baud fee is configurable from 1200-115200 thru AT command. The GSM/GPRS Modem has an inner TCP/IP stack to hook up with the internet through GPRS. SIM900A is an extremely compact and reliable wi-fi module. It is a complete GSM/GPRS module in an SMT kind and designed with a strong unmarried-chip processor integrating AMR926EJ-Score, allowing you to advantage from small dimensions and cost-effective solutions.

Arduino Mega ATmega1280 microcontroller board has 54 digital enter/output pins, 16 analogue inputs, 4 UARTs, a 16 MHz crystal oscillator, a USB connection, a power jack, an ICSP header, and a reset button. It has the entirety required to aid the microcontroller; plug it right into a PC with a USB cable or fee it with an AC-to-DC adapter or battery to get started out. The working voltage is 5V; recommended enter voltage stages from 7V to 12V but needs to know not exceed the 20V limit.

The Arduino Mega might be run by using a USB connection or an outside power supply. The electricity supply is selected automatically. External (no longer USB) charging ought to come from a battery. Leads from a battery can be inserted inside the ground and Vin pin headers of the POWER connector.

The ATmega1280 has 128 KB of flash reminiscence to keep codes (four KB used for the boot loader), eight KB of SRAM and four KB of EEPROM.

ATmega1280 has several facilities for connecting to a PC, any other Arduino, or other microcontrollers.

ATmega1280 has an applicable poly fuse that protects your PC's USB ports from shorts and overcurrent. Although most computer systems offer inner safety, the fuse gives an extra layer of protection. If greater than 500mA is applied to the USB port, the fuse will automatically prevent the connection till the fast or overload is taken away,

The venture is appealing because its uses are obvious in terms of protection and economics for the same old consumer. Furthermore, the GPS and GSM modules and the Arduino Mega are small in length, making the product usable for motors and any shifting items.

4. RESULTS AND DISCUSSION:

The prototyping circuit for the proposed tracking systems is shown in Fig. 8.

The circuit shows the hardware, including the Arduino Mega, GPS & GSM modules. The GPS module generates the vehicle location and updates the longitude and latitude, as shown in Fig. 9. The accuracy of the *GY*-GPS6MV2 GPS module is very high and goes up to almost 80%.

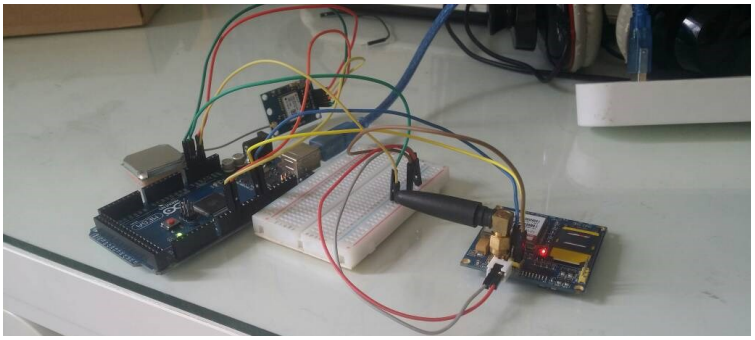

Fig. 8: Hardware prototyping circuit

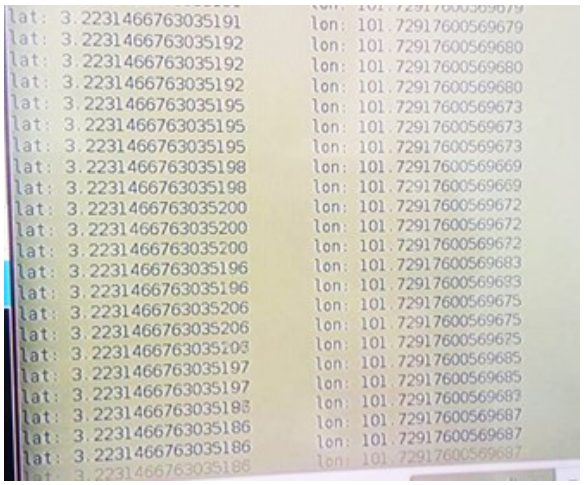

Fig. 9: Display the longitude and altitude of the Tx module

Fig. 9 shows the longitude and altitude generated by the GPS module over an hour. The GPS module then sends the data to the GSM module, sending the data to the smartphone-like in the picture below.

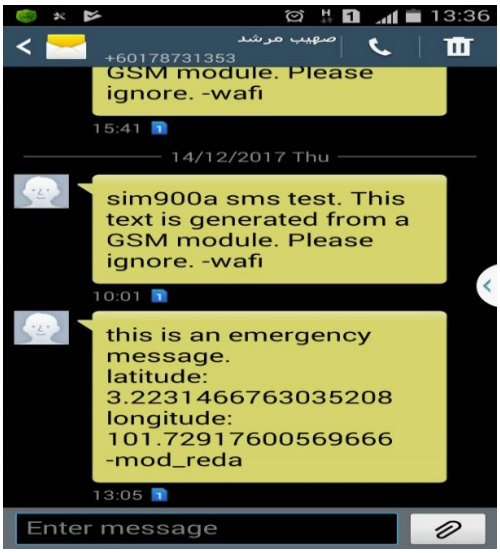

Fig. 10: SMS data

The picture in Fig.10 shows the data received as the SMS service of the mobile phone.

5. CONCLUSION

The proposed tracking and management system with GPS and GSM modules have been completed, and efficient data transmission and monitoring are experimentally verified. The project allows real-time control letting rightful applications be made. It is suggested that the use of this system will result in significant updates for vehicle tracking systems. The proposed method has multiple benefits. It could be applied for a lost car to track when dealing with the alarming vehicle management system. In the future, sensors can be used in these systems to improve their strength further. The sensors detect car mode info to the server, which could help the data process and intelligent tracking management.

The GPS and GSM technologies are implemented to reduce civilians' dangers and the extreme situation because of accidents or theft. Therefore, the ambulance or police service should take the instant step, minimizing the risks.

REFERENCES

[1] R. Rathinakumar and D. Manivannan, "Accident Information System Using GSM and GPS," Research Journal of Applied Sciences, Engineering, and Technology 4(18), pp. 3323-3326, 2012.
[2] Shirisha K and T Sivaprasad, "Acquire Bus Information using GSM Technology," International Journal of Advancements in Technology," Vol. 7(3), 2016.
[3] C. Bhanu Prakash and K. Sirisha "Design and Implementation of a Vehicle Theft Control Unit using GSM and CAN Technology," International Journal of Innovative Research in Electronics and Communications (IJIREC) Vol.1(4), pp. 46-53, 2014.
[4] Syed Ahmad Fawwaz Wafa and S. M. A. Motakabber, "IoT-Based Lab System for Teaching Methods in Times of Crisis," Asian Journal of Electrical and Electronic Engineering (AJoEEE), vol. 1(2), pp. 14 -19, 2021.
[5] N. Dhanasekar and G. Subramanian, "Accidental Navigation and Rescue System using GSM and GPS Technology," Asian Journal of Research in Social Sciences and Humanities, vol. 6(11), pp.158-166, 2016.

ASIAN JOURNAL OF ELECTRICAL AND ELECTRONIC ENGINEERING
Vol. 2 No. 1 2022
E-ISSN: 2785-8189

Investigation of the Energy Saving Capability of a Variable Inertia Magneto-Rheological (MR) Flywheel

Lihajul Islam*, Muhammad Mahbubur Rashid, and Faysal M A

Department of Mechatronics, Faculty of Engineering,
International Islamic University Malaysia

*Corresponding author: ilihajul@gmail.com

(Received:28th February 2022; Accepted: 16th April 2022)

Abstract— This research focuses on a theoretical and experimental analysis of a variable inertia magneto rheological flywheel (VIMRF). The objectives of the present study were to design and fabricate the prototype of a VIMRF and perform characteristics of energy saving capability of it. The moment of inertia has been calculated under different angular speeds and excitation currents. The prototype was designed and manufactured to verify the effectiveness of the proposed VIMRF. Simulations are primarily done to find variable characteristics of the moment of inertia of the VIMRF under certain conditions. The primary simulation shows that the moment of inertia of the VIMRF can semi-actively be tuned.

Keywords: *Magnetorheological, variable inertia, flywheel*

1. INTRODUCTION

Flywheels are showing immense promise in the field of the energy storage system. A flywheel is a mechanical device designed to store rotational energy efficiently. One topic of interest within this field is the energy-saving capability of variable inertia MR flywheel. The flywheel is an electromechanical, readily available energy storage system of rotating mass. The flywheels' size varies in size depending on the system requirements and cost-efficiency. Various research from all over the world developed a flywheel mechanism to a modern established level to cope with any system. But the fourth industrial revolution brought a new era of scientific achievement in communication, robotics, and electronics. Flywheel has been utilised for several applications, usually for energy storage or to minimise the angular velocity fluctuation of a shaft. Some energy storage applications include flywheel hybrid vehicles, cyclic alternative energy sources such as wind turbines, uninterrupted power supplies, and space power systems. The internal combustion engine, AC generators, industrial machinery such as camshafts etc., are some applications of flywheel for smoothing angular velocity fluctuations.

Within the plan of a system with a conventional flywheel utilised to minimise changes in angular velocity, the flywheel is measured on a coefficient of variance, characterised as the alter in angular velocity amid a cycle isolated by the normal angular velocity. A significant moment of inertia is required to achieve a low coefficient of fluctuation. An adjustable inertia flywheel can play a significant role in this case. Moreover, there are few research papers concerning the contribution of MR liquids within the flywheel area, which is also one of the primary reasons that trigger this extension to work.

2. RESEARCH METHODOLOGY

Over the past few decades, a wide range of work on variable inertia flywheel has been done on its energy saving capability. Jauch [1] has proposed a flywheel energy storage that is an integral part of a wind turbine rotor. Figliotti & Gomes [2] have proposed a design for a spring-connected variable inertia flywheel directly coupled to the vehicle in their study. Van de Ven [3] presents a self-governing fluidic variable inertia flywheel that can keep its angular velocity constant over a wide range of energy storage. A centrifugal pendulum in the

double mass flywheel has been adopted by Ishida et al. [4]. James et al. [5] proposed a novel self-governing fluidic variable inertia flywheel that can maintain a constant angular velocity across a range of energy storage. Yuan et al.[6] designed of a diesel generator set under the pulse load, which can replace the traditional fixed inertia flywheel of the variable inertia flywheel. Bao [7] introduced a novel type of flywheels with the variable equivalent mass moment of inertia and without a fixed connection with the input shaft to the machine. Matsuoka [8] proposed a new vibration suppression device that utilises variable inertia mass by using a fluid that acted as a series of inertia mass. But the use of magneto rheological fluid to achieve variable inertia in a flywheel has not been widely done. The energy saving capability variable inertia magneto rheological flywheel (VIMRF) in comparison to its counterparts is yet to be explored.

The research methodology starts with an extensive literature survey of the existing and ongoing works on variable inertia flywheels. Then developing a CAD design of the prototype. Following CAD design, fabricating the prototype according to the design begins. After the prototype is fabricated, the testing phase starts. The final step is to perform experiments to find the energy saving characteristics of the VIMRF.

2.1 Design of the Variable Inertia Magneto-Rheological Flywheel

2.1.1. Modelling of variable inertia flywheel

The inertia of the flywheel varies as the slider moves through the slot in a variable inertia flywheel. When the flywheel speed is zero, the springs are at their full length in the extended position, touching the hub. Gravity isn't taken into account here. The springs can only be compressed and not extended any farther. The slider's moment of inertia around its own mass centre and the fixed structural part's moment of inertia around the shaft centre are both expressed as

$$J_s = \frac{1}{4} m_s \left(\frac{d_s^2}{4} + \frac{l_s^2}{3} \right),$$

Where m_s, d_s, l_s and Ns = 4 are the slider mass, slider diameter, slider length and number of slots, respectively, Jscd = 12mscd(ri2 + ro2) is the polar moment of inertia of a solid flywheel of uniform thickness, m_{scd} is its mass, J_{shaft} is the polar moment of inertia of the shaft, and r_i and r_o are the inner and outer radius of the circular disk, respectively, and the lost inertia of the removed material from each rectangular slot

$$J_{slot} = m_{slot} \left\{ \frac{1}{12} \left(d_s^2 + l_{slot}^2 \right) + \left(r_o - 0.5 l_{slot} \right)^2 \right\},$$

where m_{slot} and l_{slot} are the mass of the removed material from each slot of the circular disk and the length of the slot, respectively. The slider moves along the slot while it rotates along with the flywheel. The equation of the motion of the slider can be obtained using Lagrange's approach. The Lagrangian is expressed as

$$L = T - U$$

where T and U are the kinetic and potential energy of the variable inertial flywheel, respectively. The kinetic energy can be formulated from radial and tangential velocity components of the ith slider, l_i and li$\dot{\theta}$, respectively, as

$$T = \frac{1}{2} \sum_{i=1}^{4} m_s \left(\dot{l}_i^2 + l_i^2 \dot{\theta}^2 \right) + \frac{1}{2} \left(J_f + 4 J_s \right) \dot{\theta}^2,$$

where $\dot{l}$i and $\dot{\theta} = \omega$f are the instantaneous linear velocity of the ith (i = 1.0.4) slider and angular velocity of the flywheel, and J_f is the flywheel's polar moment of inertia, respectively. The slider's potential energy U is introduced as well as the Rayleigh dissipation function D for resistive losses, ignoring gravity.

$$U = \frac{1}{2} \sum_{i=1}^{4} k_{fs} \left(l_i - l_{\min} \right)^2$$

$$D = \frac{1}{2} c_\theta \dot{\theta}^2 + \frac{1}{2} c_{line} \dot{\theta}^2 + \frac{1}{2} \sum_{i=1}^{4} c_l \dot{l}_i^2,$$

where k_{fs}, is the spring stiffness of the variable inertia flywheel, l_{min}, denotes the free length of the spring, c theta is the combined viscous damping co-efficient for loss at the bearings and viscous drag on the flywheel, c_{line} is the coefficient of line resistance of the circuit and cl is the viscous damping between the slider and the

slot. The radial and tangential components of acceleration of the ith slider are a r = ¨li - li$\dot{\theta}$ 2 and aθ = 2$\dot{l}$i$\dot{\theta}$ + li$\ddot{\theta}$, respectively. The normal reaction on the slot from the slider is m_{sa} and this reaction gives a part of the load torque. The Lagrange's equations of motion in generalised coordinates are given as

$$\frac{d}{dt}\left(\frac{\partial L}{\partial \dot{l}_i}\right) - \frac{\partial L}{\partial l_i} + \frac{\partial D}{\partial \dot{l}_i} = F_{ci},\ i = 1 \ldots 4;$$

$$\frac{d}{dt}\left(\frac{\partial L}{\partial \dot{\theta}}\right) - \frac{\partial L}{\partial \theta} + \frac{\partial D}{\partial \dot{\theta}} = T_m - T_l,$$

2.1.2. Flywheel design

MR variable inertia flywheel and inner structure are shown in Figure 1. The MR variable inertia flywheel consists of a frame and four magnetorheological dampers with four identical slots. Each damper includes a cylinder, piston, MRF and spring. The middle of the frame is provided with a hole and a keyway for fixing the connection with the rotating shaft. The frame is set in a radial direction with four rectangular grooves and the cylinder is settled in the rectangular groove of the frame. A pre-compressed spring is set between the piston and the frame. The coil is entangled in the double ring groove of the piston. The non-woven fabric with MRF is placed in the gap between the piston and cylinder. Nonwoven fabrics are made from hygroscopic fibres and can store MRF. Its structural principle is like that of magnetorheological foam, which can simplify the damper structure and avoid leakage of MRF without sealing.

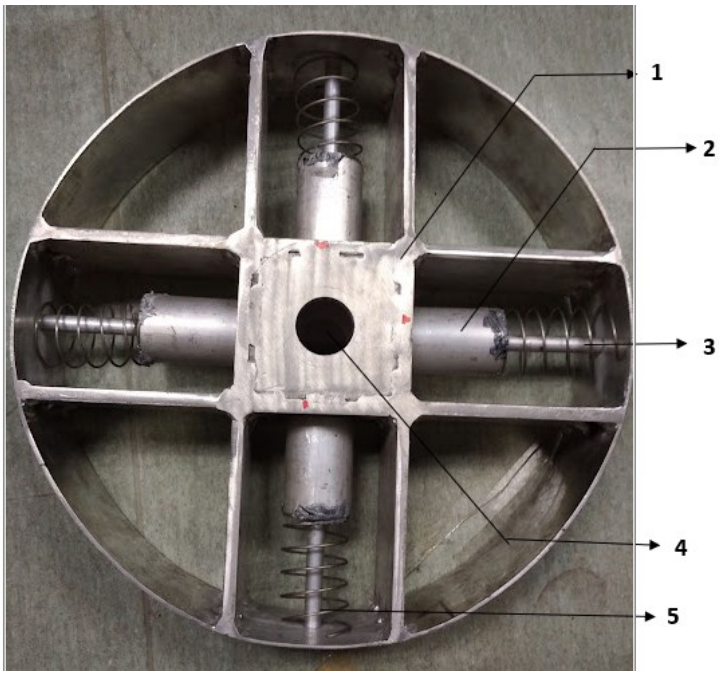

Fig. 1. Prototype of the flywheel (1) Rim of the block, (2) Mass block, (3) Spring, (4) Shaft hole and (5) Mass holding rod

2.2. Experimental Setup

This experiment involves the fabrication of a variable inertia magneto rheological flywheel (VIMRF). The design consists of four MR dampers used to adjust the rotational inertia of the flywheel. The flywheel will relate to the induction motor. An inverter will control the induction motor. A torque sensor will be placed between the motor and flywheel to obtain the experiment's output. Below is the schematic diagram of the system.

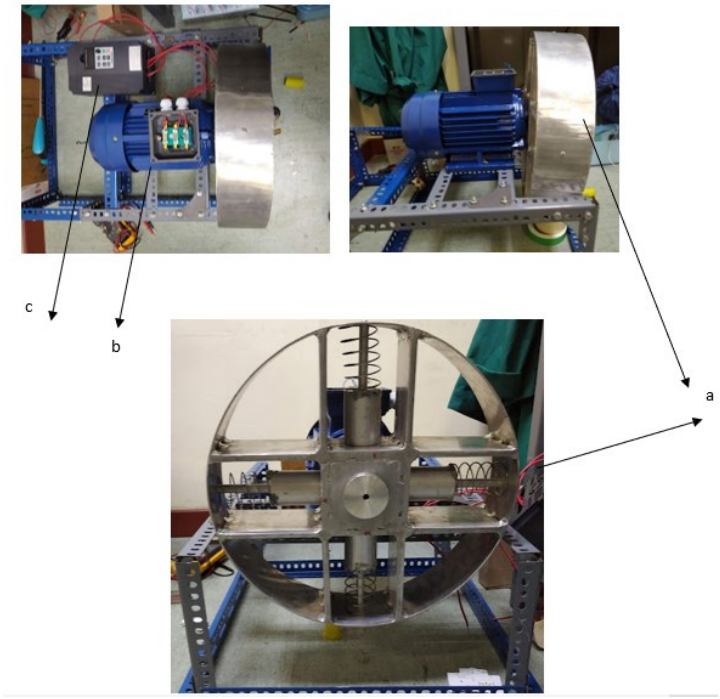

Figure 2 Experimental setup of the flywheel (a) Variable inertia flywheel, (b) Induction Motor, (c) Inverter

2.3 Results

The speed control system of the AC motor with VIF has been simulated using MATLAB. VIF is represented as an energy storage device in the internal feedback loop. VIF adjusts the system by releasing stored kinetic energy when the load torque increases. VIF will absorb excess energy from the system as load torque decreases. The constructed feedback loop uses the motor's angular acceleration as an input signal, and its output minimises the loading pulse impact. number.

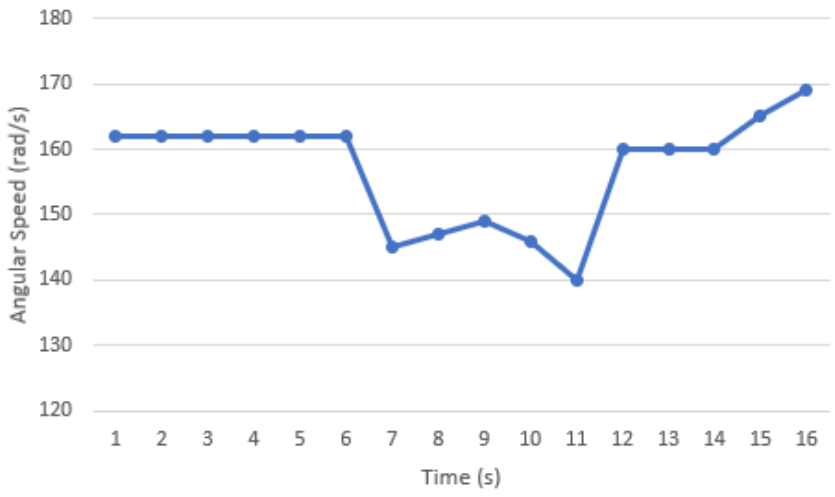

Fig 3 Angular speed of the motor(rad/s)

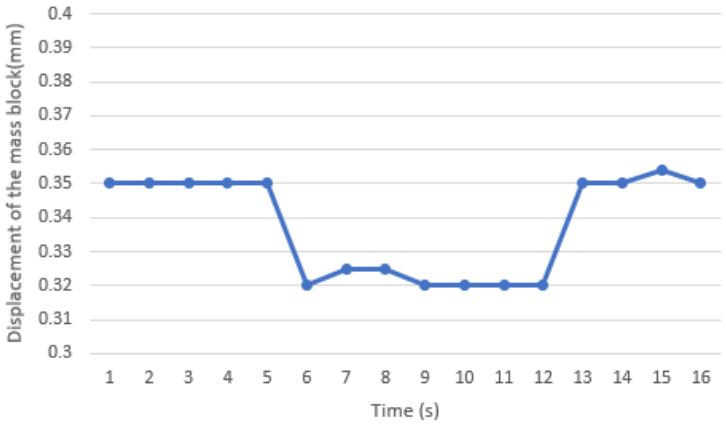

Fig 4 Displacement of the mass block(mm)

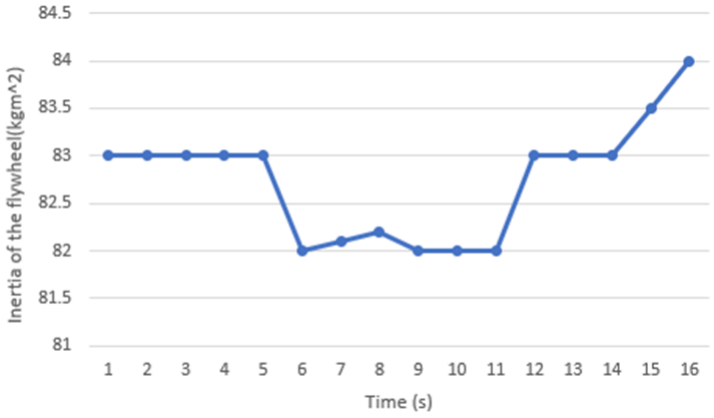

Fig 5 Inertia of the flywheel(kgm^2)

The Flywheel's Variable Behavior Equivalent Mass m_a and Moment of Inertia I_{af}, With the input velocity, the equivalent mass ma will change. However, when the rotating speed is very low, the slider will remain in its initial position, and ma will be the smallest number. The spring in the slot will fully compress when the rotating speed reaches a specific threshold, and ma will reach its maximum value. To study the flywheel's overall behaviour, the input signal should be chosen so that the sliders do not stay at the two ends of the slot and are neither the minimum nor the maximum value. Because the sinusoidal velocity input signal with a frequency of 0.1 Hz and an amplitude of 0.0314 m/s is less sudden than the rectangular and triangular inputs, it is employed. This is also because the sliders will travel over the majority of the travel range in the slots when given a sinusoidal input of this frequency and amplitude. As a result, the change in equivalent mass can be noticed over a larger range of values. The varied position of the sliders, the variable moment of inertia, and the equivalent mass of the flywheel in response to the sinusoidal input (Fig. 6) are all shown in reaction to the sinusoidal input. Figures 7–9 depict the results, respectively. The moment of inertia and equivalent mass of the flywheel vary adaptively in response to the input, as seen in Figs. 8 and 9, but the variation frequency is doubled.

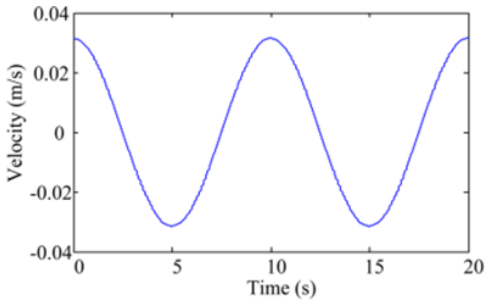

Fig. 6 Sinusoidal velocity input (frequency 5 0.1 Hz, amplitude 5 0.0314 m/s),

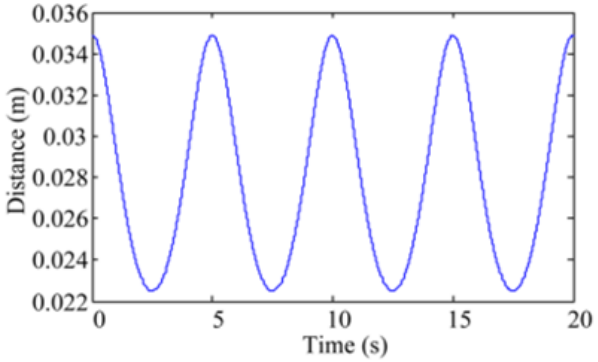

Fig. 7 Slider location that varies in response to the velocity input in Fig 6,

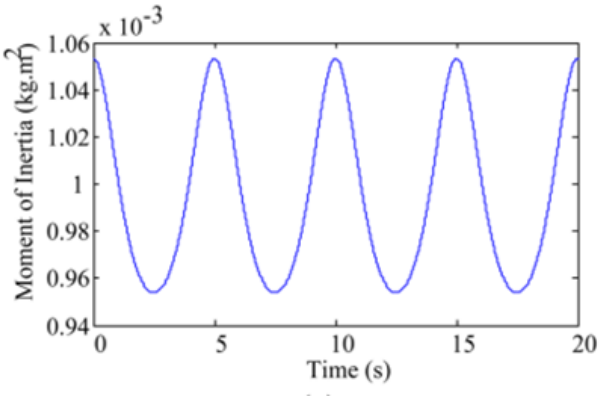

Fig. 8 The variable moment of inertia of the flywheel associated with the slider location presented in Fig. 7,

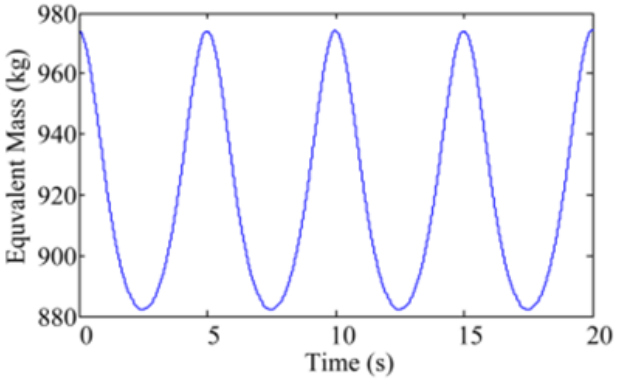

Fig. 9 The variable equivalent mass of the flywheel due to the location change of the sliders.

Figure 10 depicts the centrifugal force, spring tension, mass block displacement, and inertia curve as a function of rotational speed. The centrifugal force, displacement, and spring tension change slowly when the speed is less than 1000 RPM in the first column. However, when the speed exceeds 1000 RPM, the quadratic equation values increase, indicating that the flywheel has a greater energy storage capacity at high speeds. The effect of gravity on the centrifugal force and friction in the second column is represented by positive and negative alternating high frequency signals so that gravity can be ignored. The normal force from the gravity of the mass block produces coulomb friction, and the friction surface varies in 360 degrees, resulting in a positive and negative alternating high frequency signal. Because the angular acceleration of the flywheel is constant at 1500 RPM, the friction created by mass block inertia is also constant, as seen in the third photo of the second column.

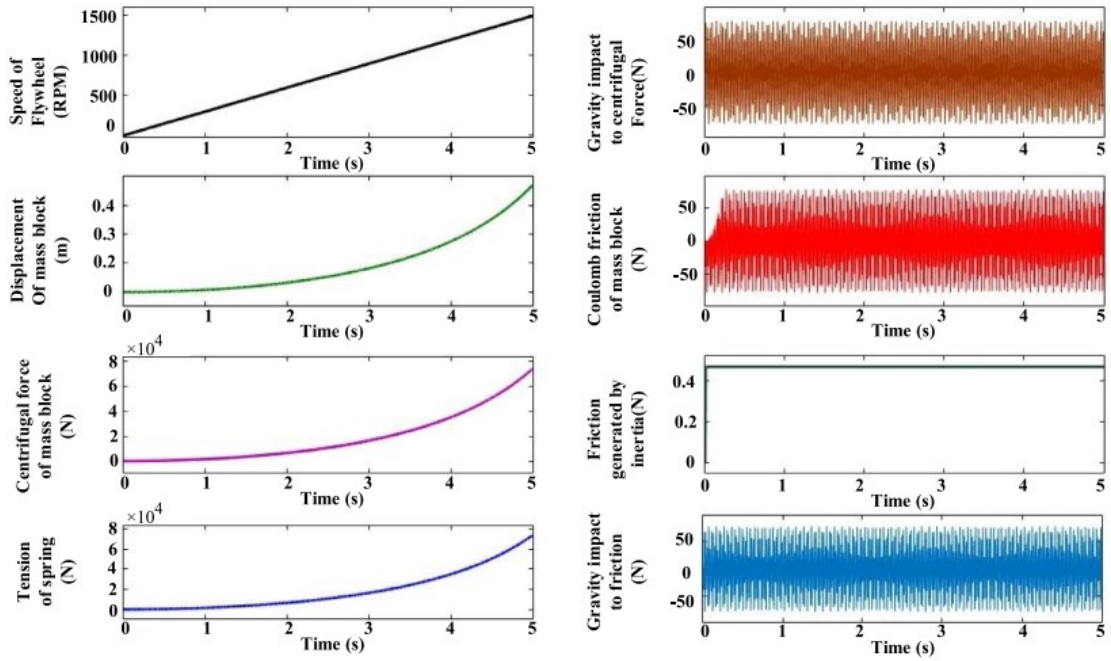

Figure 10. Simulation diagram of the flywheel

3. CONCLUSION

The objective of this research was to fabricate a prototype of VIMRF, do a simulation of the system and analyse and perform characteristics of energy saving capability of the VIMRF. The idea of storing energy in the rotating mass of a flywheel looks to be particularly enticing because of its simplicity. Closer inspection, however, reveals intricacies that make deploying an operating system significantly more challenging. One of the most challenging difficulties is transferring energy to and from the energy storage flywheel. This study looks at some of the research done on the topic of variable inertia flywheels. The experimental results are on good terms with the simulation results.

REFERENCES

[1] Jauch, C. Controls of a Flywheel in a Wind Turbine Rotor. Wind Eng. 2016, 40, 173–185.
[2] Figliotti MP and Gomes MW. A variable-inertia flywheel model for regenerative braking on a bicycle. In: ASME 2014 dynamic systems and control conference, San Antonio, TX, 22–24 October 2014, paper no. DSCC2014-6276. New York: American Society of Mechanical Engineers.
[3] Van de Ven J. Fluidic variable inertia flywheel. In: 7th international energy conversion engineering conference, Denver, CO, 2–5 August 2009, paper no. AIAA2009- 4501. Reston, VA: American Institute of Aeronautics and Astronautics.
[4] Ishida Y I T, Fukami T and Ueda M 2009 Torsional vibration suppression by roller type centrifugal vibration absorbers Journal of vibration and acoustics 131 1-10.
[5] James V D V 2012 Fluidic variable inertia flywheel and flywheel accumulator system. US
[6] Yuan L G, Zeng F M and Xing G X 2010 Research on the design and control strategy of variable inertia flywheel in diesel generator unit under pulsed load. International Conference on Computing, Control and Industrial Engineering 187-9
[7] Bao E, Hu H Y and Liu D Y 2011 The theory and synthesis of high effect flywheel with variable equivalent mass moment of inertia Advanced Materials Research 199-200 225-31
[8] Matsuoka T 2011 Vibration suppression device having variable inertia mass by MR-fluid. ASME 2011 International Design Engineering Technical Conferences and Computers and Information in Engineering Conference 1181-5

ASIAN JOURNAL OF ELECTRICAL AND ELECTRONIC ENGINEERING
Vol. 2 No. 1 2022
E-ISSN: 2785-8189

Optimisation of Energy Efficiency of Three-Phase Induction Motor Drives for Industrial Applications

Alshaikh Abdallah, Tahsin F H
Department of Mechatronics, Faculty of Engineering,
International Islamic University Malaysia

*Corresponding author: tahsin10797@gmail.com

(Received:28th February 2022; Accepted: 18th April 2022)

Abstract— Electric motors are used in nearly 60% of the global electrical power generated. Due to the greater energy consumption, there has been a considerable rise in production costs and environmental degradation, increasing general operating expenses. Therefore, the efficiency of three-phase squirrel cage induction motors (SCIMs) may be improved to save a large amount of electricity. The thesis aims to investigate increasing the efficiency of three-phase (SCIM). The proposed method improves the efficiency of (SCIMs) using PID controller Simulink design in Simulink/MATLAB. To successfully determine the motor characteristics and simulate a three-phase (SCIM) under various loads. The effects of lowering the voltage and using PID controller on motor characteristics such as generated torque, power factor, reactive power, apparent power, output power, rotor speed, and magnetising current are also discussed. The simulation result found that the proposed motor efficiency and power factor method is improved by using a PID controller. At motor torque of 12 N-m, the efficiency is 80%, which rises to 92 % at higher motor torques. After applying the proposed method, the power factor becomes 0.64%, which is an improvement of 0.2%.

Keywords: *SCIMs, Induction motors*

1. INTRODUCTION

The three-phase induction motors are most employed or used in what is known as industrial settings since mechanical energy is derived from electrical energy. Today, electric industries such as automotive factories use approximately 69% of electric power. And these electric drives are primarily alternating current (AC) and direct current (DC). In the last forty years, the popularity of the AC drives grew significantly, particularly the three-phase induction motor drives, which offered more robustness, efficiency, performance, and an incredible sustainable structure that is utilised mainly in industrial applications—for instance, powering elevators, refrigeration systems, robotics, and so on.

Since the development of the first induction motor by Nikola Tesla in the nineteenth century, the universal property of motors, regardless of their purpose, is that a large amount of electricity is needed to operate. The structure and performance of induction motors have since significantly improved. Specifically, this has been executed via motor power losses decrease by adopting high conductivity materials. For example, this may include using copper instead of criterion steel in the squirrel cage rotor. The stator core is also shaped using silicon steel sheets, which minimises the hysteresis losses and the eddy currents. [1]

The process control techniques in the industrial field have witnessed significant advances in the last few decades. Various control systems and methods, such as Neural and Fuzzy logic control, have been under study and investigation. In relation to these, the most well-find is the Proportional Integral Derivative (PID) controller because it is extensively employed and utilised due to the fact that its structure is quite simple and its performance is very robust and durable under a wide area of operating situations. However, it has been considered hard in terms of tuning PID controllers' gains because numerous industrial plants had to face several issues such as large orders, time delays, and nonlinearities. [2]

2. RESEARCH METHODOLOGY

Based on Essensa and Christian [4], electric motors are used in almost sixty per cent of the global electrical power generated. Because of greater energy consumption, there has been a significant rise in production costs and environmental degradation, increasing general operating expenses. Induction motor driving systems that are more efficient and dependable are critically required for current and future applications. This study aims to develop an induction motor with low manufacturing and operating costs and with significant operational efficiency.

The investigated project aims to achieve a method to obtain high efficiency for a three-phase induction motor using PID controller Simulink design in Simulink Matlab. Therefore, the project's methodology is to compare three-phase induction motors under various loads in normal operation (at rated voltage) without using PID controller and Simulink various loads using PID controller to find the highest efficiency.

2.1 Simulink Model of Three Phase Induction Motor by without Using PID controller under Different Loads

A Simulink model was constructed to compare the standard operating procedure to the three-phase SCIM technique (see Figure 1). To connect the three-phase SCIM stator coils, spliced Y connections are employed. The excitation of the DC generator is used to provide the AC generator loads (rotor-shaft-rotor-shaft-rotor-shaft). Simulink represents a generator as an adverse torque signal in a DC or AC machine. As a result, the applied load torque must be positive, implying a one-ton increase in the dc generator's torque. It's wired into a dc generator with a variable resistive load. The standard practice is to adjust the resistive load while maintaining the motor's rated voltage. As a result, the engine is always under stress. To guarantee optimal efficiency at rising speeds, the voltage supplied to the motor may be varied in a predetermined way (rated voltage). Voltage and current, power factor, apparent power, rotor speed, and active and reactive power are all measured using the model's various blocks.

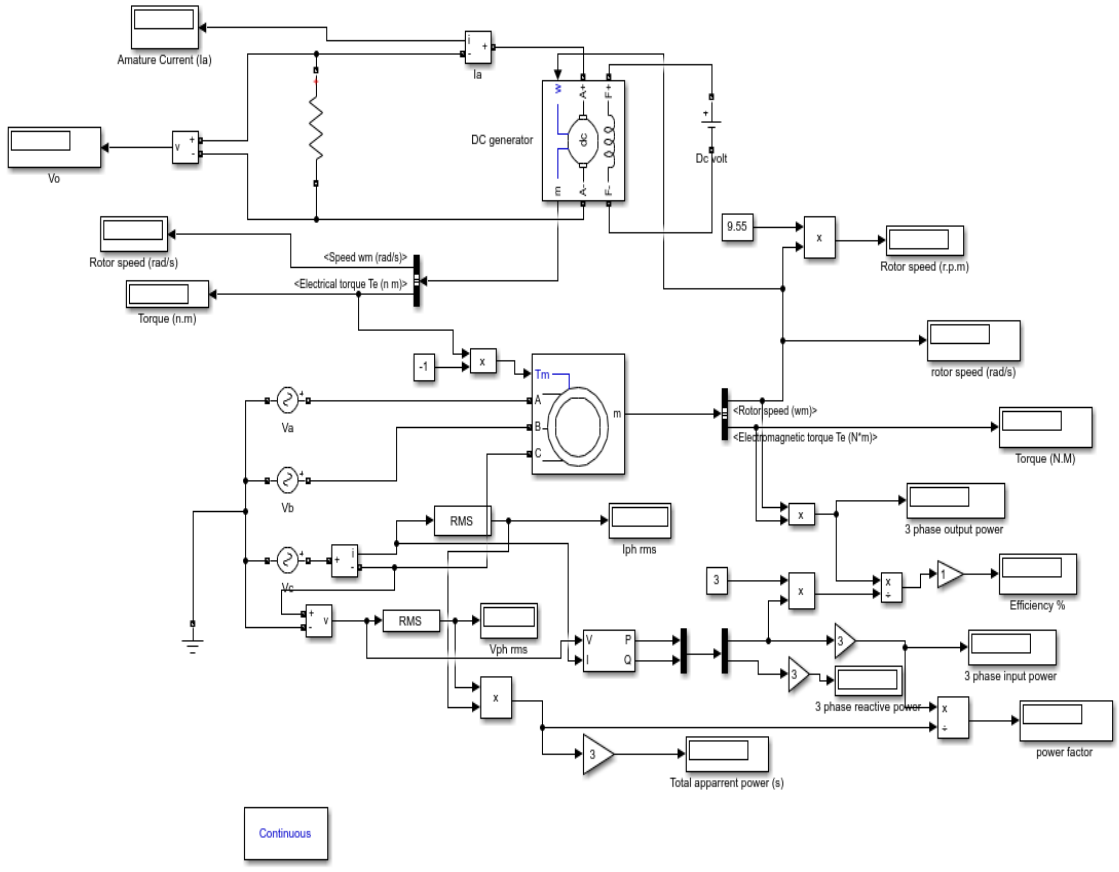

Fig 1 Simulink model of three-phase induction motor without PID controller [3]

2.2 Proposed Model of Three Phase Induction Motor by Using PID controller under Different Loads:

For example, in the industrial sector, DC generators may be used in servo systems and speed control. Due to the PID controller's simplicity, robustness, and ability to be tuned. The PID controller-based Simulink model in Fig. 2 compares the SCIM technique with normal operation. The stator windings are connected in a Y-connection using a three-phase SCIM concept. There is an ac generator attached to the motor's shaft, and the ac generator itself is linked to the dc generator using a direct connection. It is possible to use a PID controller in Simulink to regulate the output voltage serving as a generator. This results in a model where the applied load torque to the motor exceeds the dc generator torque. A changing resistive load charges the dc generator. By setting the applied voltage to the motor's rating, the load on the motor may be adjusted by varying resistance in the load. Using the suggested approach, the PID controller applied on speed is changed to operate at maximum efficiency more significantly than regular operation. There are various blocks in the Simulink for measuring various variables such as stator current, the voltage (V), active power (W) and reactive power (W), efficiency(%), as well as output power, apparent power and rotor speed.

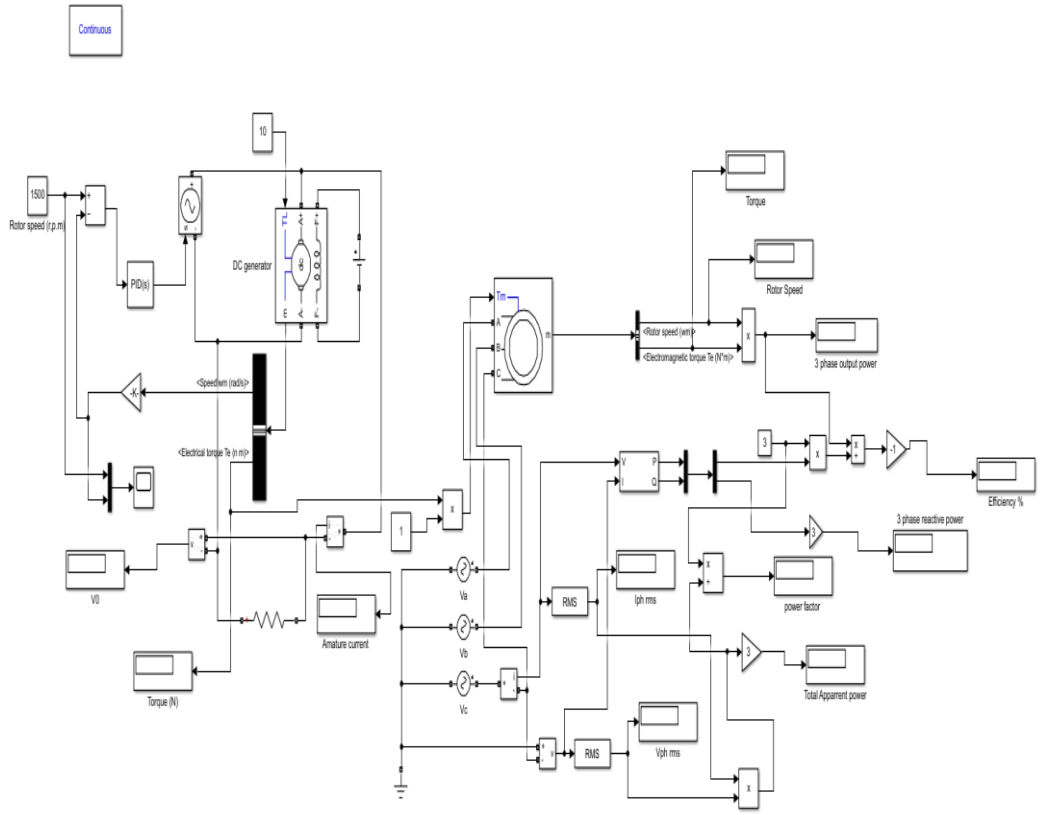

Figure 2 Simulink model of three phase by using PID Controller

2.3 The result of Simulink of a three-phase induction motor under various loads with using PID controller

After switching the MATLAB/Simulink with the PID controller, various characteristics are provided to illustrate their change with motor torque in normal operation and the suggested technique. As a result, the motor's applied voltage is maintained at its rated value. PID controllers are extremely effective and powerful controllers with a superior control strategy for maintaining motor speed. PID controller parameter values are set using tuning procedures and shown in Figures 3 and 4. Motor efficiency, power factor, output power, perceived power, stator current, and rotor speed are several parameters. Simulations of the suggested speed control model were carried out using Matlab's Simulink platform. This section shows the simulation outcome of a DC generator with motor speed control against the impact of load with speed – Torque characteristic curve. On the Simulink platform, a block scheme of a system model, whether without or with a PID regulator, is generated. To

begin, the step response of the system model with a PID regulator is calculated and shown in figure 4. The rising time is 1.2 seconds, with a 2-second settling period. The steady-state error accounts for around 90% of the final result. We can see that when the motor is operating at optimum efficiency, the stator phase current is lower than when the motor is operating at light loads. The applied voltage is lower than the rated voltage. Reduced voltage boosts stator current and reduces motor effectiveness when the motor torque exceeds typical operating torque.

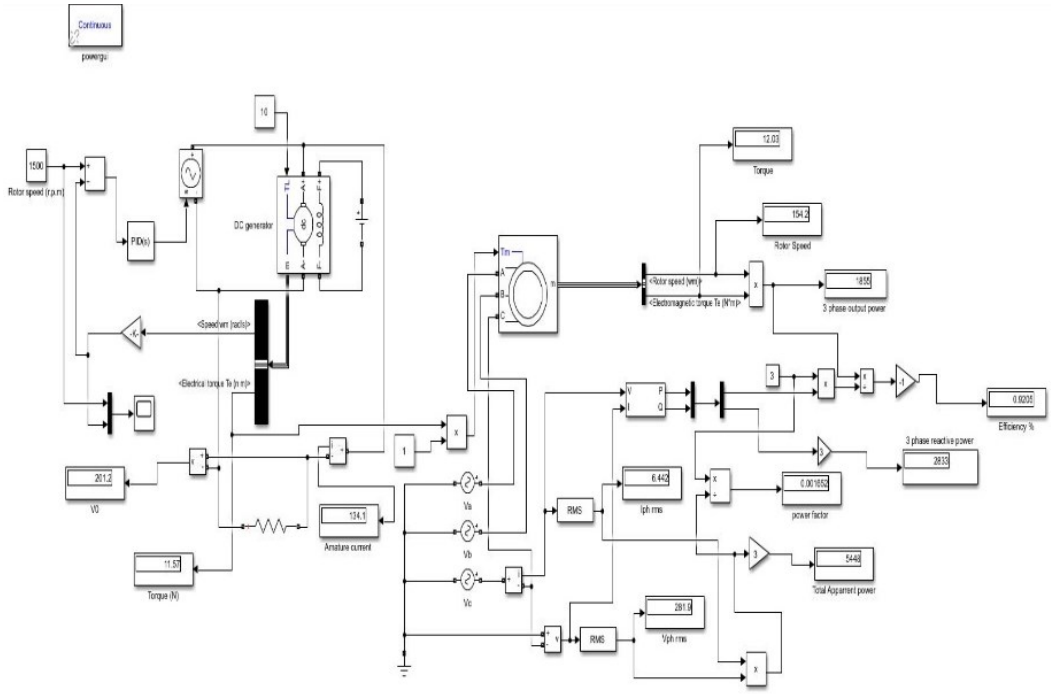

Figure 3 Simulink outcome of three phase by using PID Controller

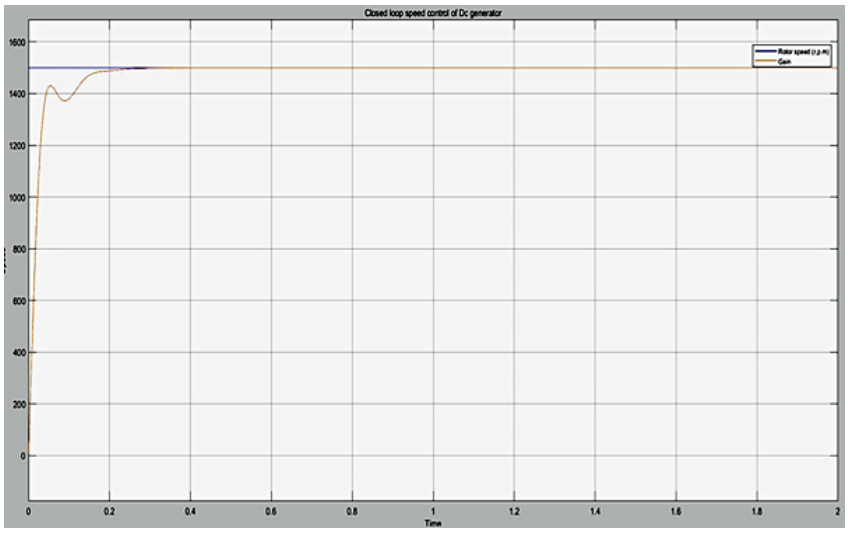

Figure 4 Result of controlling Rotor Speed by using PID Controller.

2.4. Data Collection for Results Simulation under Different Loads

Industrial variable speed implementation, which has the most requesting speed-torque characteristics, is straightforward to control. It is essential to apply PID controllers when the loads vary. A PID controller was used to regulate the speed of the motor while it was under load. As the motor speed remains constant, the load torque may be changed. The approach that was proposed was well thought out and thoroughly tried. For a

motor's open-loop speed regulation, the PID controller proved to be very effective and powerful, as shown by the experiment results. PID controller parameter values were set using the Custom Tuning process. Based on simulation findings, the PID controller is a better choice for regulating and maintaining the speed of a motor under a variety of load circumstances. Researchers found that a PID-based closed loop speed control system was effective even with load disruptions. The motor's efficiency and power factor may be enhanced and maintained by lowering the applied voltage while running at a speed that can be controlled. The applied voltage may be reduced if the stator current and perceived power are low. As a result, the engine's lifespan is extended, and power is saved.

Figure 5 shows that the stator phase current fluctuates with motor torque. The stator phase current is lower when the motor runs at optimum efficiency than when a PID controller controls the motor. The voltage applied is lower than the rated voltage. It is possible to improve motor efficiency by applying voltage for increasing the stator current while the motor is operating at a higher motor torque than typical. Therefore, the motor's rated voltage is maintained.

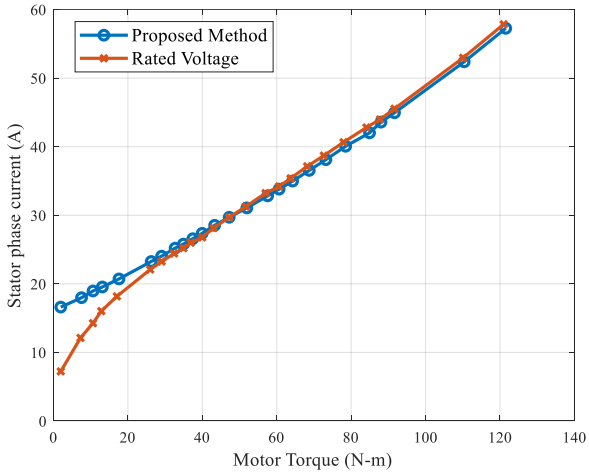

Figure 5 Outcome Simulink of stator phase verse motor torque

Figure 6 depicts the variation in motor efficiency as a function of motor torque. In normal operation, the applied voltage fluctuates at various rates below the rated value in order to hold the motor's efficiency at optimal efficiency at all loads (rated voltage). The efficiency of motors with more significant torques than the motor torque at optimum efficiency in the normal process is reduced when the applicated voltage is decreased, as can be shown. This necessitates that the rated voltage be maintained.

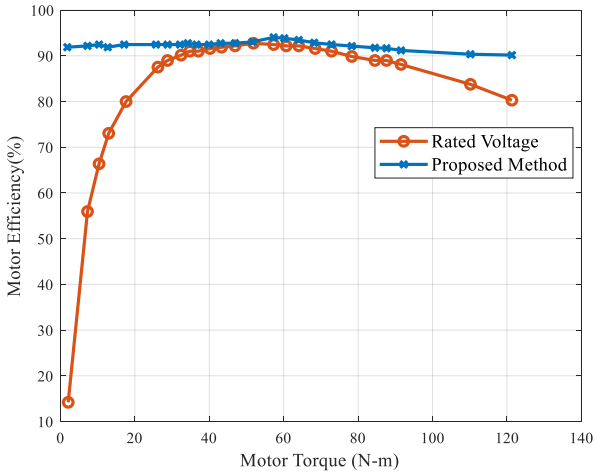

Figure 6 Outcome Simulink of Efficiency verse motor torque

The link between managing the rotor speed using a PID controller and motor torque is seen in Figure 7. With loads, the motor is operated at a steady speed, with the applied voltage reduced to maximise efficiency. As can be seen in this graph, the rotor speed is set to switch the motor at optimal performance. Consequently, the rotor speed is still controlled appropriately for the driving load. When a centrifugal pump is working at maximum efficiency, it's vital to make sure that reducing the speed doesn't result in inadequate fluid flow.

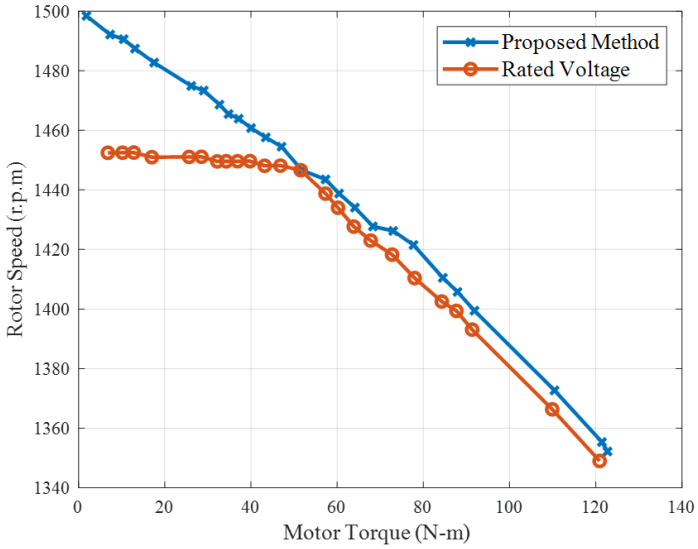

Figure 7 Outcome Simulink of Rotor speed (r.p.m) verse motor torque

The fluctuation of apparent and reactive power as a function of motor torque is shown in Figures 8 and 9. As can be seen, the proposed strategy of apparent and reactive power is less than normal operation by regulating speeds. When the current is increased, it is evident that the apparent and reactive power at loads drops. The magnitude of the voltage drop is larger than the magnitude of the current increase, resulting in an apparent power loss. To prevent outflow current more than the rated current and a drop in apparent and reactive power at the load, the applied voltage must be improved at the same rate as the current increases.

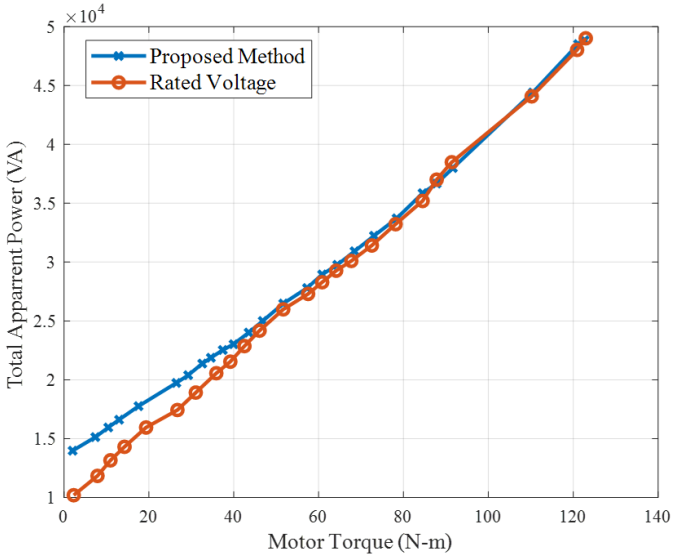

Figure 8 Outcome Simulink of Total Apparent power verse motor torque

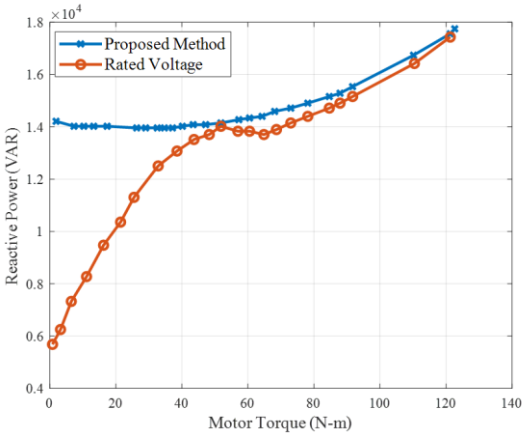

Figure 9 Outcome Simulink of Reactive power verse motor torque

Figure 10 depicts the variation in output power and motor torque. The output power of the suggested approach for managing speeds with varying loads is lower than the rated voltage, as can be shown. In light and heavy load operation, the rotor speed is controlled because the applied voltage is reduced below its rated value

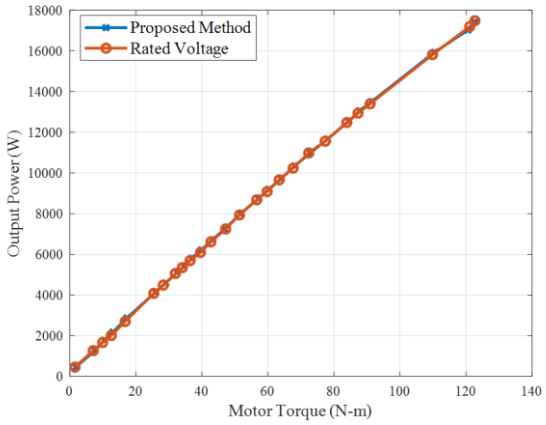

Figure 10 Outcome Simulink of Output power versus motor torque

In order to achieve the required speed, the PID controller was used in the existing block diagram of the system model in this experiment. After that, the system model was evaluated under full load without using a PID controller. Figure 7 depicts the speed-torque step response. The pace isn't up to par with the expected benchmark. The graph also shows that the load torque changes from 1000 to again. A PID controller is utilised to solve the existing challenge of speed control under load. Figure 4 illustrates the simulation graph of the system model. The system's responsiveness improves in terms of target speed sustainability with zero load torque when the same PID controller parameter values are used. However, when the load torque increases from 1000 to 1500Nm, the speed sustainability decreases dramatically. As seen in this graph, the speed is considerably reduced using closed loop speed control under full-load conditions, and the efficiency is over 90%.

3. CONCLUSION

A **STANDARD** method of converting electric power into mechanical energy is **USING** three-phase induction motors. Three-phase induction motors consume most of the electricity utilised in the sector. Motors with these specifications have a low-efficiency rating and power factor while running at typical loads. To preserve energy, high power factors and efficient motors are required. By improving efficiency under various loads, it is possible to test the influence of the suggested technique on motor properties such as stator current, output power, reactive power, rotor speed, and others.

To increase motor efficiency, a simple and inexpensive solution has been presented. The SCIM efficiency

stays constant at its maximum value while the motor runs at a higher speed than usual. In both conditional situations, the stator current is inversely proportional to the rotor speed. Its highest value is at the beginning of the cycle (when slip equals one) and its lowest value is after the cycle. To put it simply, the stator's value is equivalent to zero load current. When the motor's constant losses are equal to its variable losses, it operates at its optimum efficiency. Any load rise leads to a rise in power losses, so the efficiency declines beyond the maximum efficiency threshold. Because there is no output power, the efficiency decreases indefinitely. Motor efficiency and power factor are improved by using Fig. 4.4; at motor torque of 12 N-m, the efficiency is 80%, which rises to 92 % at higher motor torques. After applying the proposed method, the power factor becomes 0.64%, which is an improvement of 0.2%.

REFERENCES

[1] J. Resa, D. Cortes, J. F. Marquez-Rubio, and D. Navarro, "Reduction of induction motor energy consumption via variable velocity and flux references," Electron., vol. 8, no. 7, pp. 1–14, 2019, doi: 10.3390/electronics8070740

[2] K. Lu, W. Zhou, G. Zeng, and W. Du, "Design of PID controller based on a self-adaptive state-space predictive functional control using extremal optimisation method," J. Franklin Inst., vol. 355, no. 5, pp. 2197–2220, 2018, doi: 10.1016/j.jfranklin.2017.12.034.

[3] Sekaran et al., Title," Pakistan Res. J. Manag. Sci., vol. 7, no. 5, pp. 1–2, 2018.

[4] Bakshi, M. B. U. (2009). Transformers & Induction Machines. Technical Publications

ASIAN JOURNAL OF ELECTRICAL AND ELECTRONIC ENGINEERING
Vol. 2 No. 1 2022
E-ISSN: 2785-8189

Multivariate EEG Signal Processing Techniques for the Aid of Severely Disabled People

Muhammad I. Ibrahimy[1*], and Ahmad I. Ibrahimy[2]

[1]*Faculty of Engineering, International Islamic University Malaysia, Kuala Lumpur, Malaysia*
[2]*Faculty of Economics and Business, Universiti Malaysia Sarawak, Sarawak, Malaysia*

*Corresponding author: ibrahimy@iium.edu.my

(Received:18th March 2022; Accepted: 18th April 2022)

Abstract— Electroencephalography (EEG) has been used for several years as a trace of signals for facilitating subjects with serious infirmities to communicate with computers and other devices. Many studies have revealed the correlation of mental tasks with the EEG signals for actual or fictional movements. However, the performance of Brain Computer Interface (BCI) using EEG signal is still below enough to assist any disabled people. One reason could be that the researchers in this field (motor imagery based BCI) normally use two to three channels of EEG signal. This might limit the performance of BCI, as an extra source of information generally helps in detecting a person's motor movement intentions. Therefore, the proposed research work is involved with three or more channels of EEG signal for online BCI. Two fundamental objectives for BCI based on motor movement imagery from multichannel signals are aimed at in this research work: i) to develop a technique of multivariate feature extraction for motor imagery related to multichannel EEG signals; and ii) to develop an appropriate machine learning based feature classification algorithm for Brain Computer Interface. Nevertheless, all other problems like interfacing and real-time operations with current BCIs are also addressed and attempts are made to reduce the problems. The methodology can be described by following steps as follows: i) at least 3 channels of EEG signal are recorded; ii) a few features are extracted from preprocessed EEG signal; iii) all extracted features are classified to generate commands for BCI; iv) finally evaluate the performance of the proposed algorithm for BCI. The challenge of this research work is to investigate and find an appropriate model for online (real-time) BCI with a realistic performance to be made in achieving better lives for people with severe disabilities in Malaysia and abroad.

Keywords: *Electroencephalography, Brain Computer Interface, Motor Imagery EEG, and Cohen's Kappa*

1. INTRODUCTION

Many studies have revealed the correlation of mental tasks with the EEG signals for actual or fictional movements. Current BCIs mostly concentrate on signals from extends of the cortex that is likely to demonstrate activity that is directly linked to a particular type of intention (e.g., movement intention). Though, the well-off interconnectivity between different cortical extends may permit events in one area to be preceded or accompanied by detectable patterns in other distinct areas. This fact has only been narrowly explored in relation to BCIs. Hence, the main objective of this research work is to investigate the functional time-related cortical interconnectivity both as an alternative and as an additional source of information for detecting a person's motor intentions within EEG signals.

An additional source of information generally helps in detecting a person's motor movement intentions; thus, the proposed research work is aimed to involve three or more channels of EEGs for online BCI. Though with a higher number of EEG channels and a higher degree of signal processing technique may yield a quicker latency than what is available currently, the challenge of this research work is to investigate and find an appropriate model for online (real-time) BCI.

2. MOTIVATION

A person with disabilities is being given protection under the law of Persons with Disabilities Act 2008 in Malaysia. This act includes habilitation and rehabilitation as well as the development of the quality of life and well-being of individuals with serious disabilities.

Brain Computer Interface (BCI) is a system that establishes a direct interaction path between the brain and an outside device. It is often designed to aid, intensify or restore human cognitive or sensory-motor functions. The conception of BCI is not very new but still in its earliest research stages and has vast scope to explore. US, Europe, Japan and even neighbor country Singapore is doing research on BCI and neuro-informatics, but Malaysia is far behind in doing so. Few groups in Malaysia have started work in BCI, but no group is working in motor imagery related BCI so far. On the other hand, very few research groups are available in Malaysia that work on EEG signal analysis. Therefore, this research is to be made to achieve better lives for individuals with serious disabilities for fulfilling the needs and rights of disabled people, especially in Malaysia.

3. REVIEWS

A Brain Computer Interface (BCI) creates a direct interaction channel between a human brain and a control or interaction device without involving neuro-muscular paths [1]. Such user interfaces can be extremely beneficial to individuals with complete dysfunction of the neuromuscular system. To effective use of a BCI, the user should generate various brain activities that will be recognized by the system and translated into commands to control outside devices such as computers, wheelchairs etc. The development of a BCI implies three functions: (i) recording of the cerebral (brain) signal, e.g., EEG; (ii) extraction of mental task related features or information from the recorded signal; and (iii) translation (classification) of the extracted information to a control command [2].

Research on Human Brain Map explains the association of brain segments with every physiological or mental action. Sensory and motor homunculus are the representation of the body parts to every segment of the brainpower. Hence, for every key EEG rhythm and for a collection of induced capabilities, the sites and mechanisms of initiating EEG and their relations with particular aspects of brain work are no longer entirely obscure [3]. The imagery of motor progress could be identified from non-invasive EEGs by arranging electrodes (with a brain cap) around the motor and sensory cortex fields of the subject's scalp [4]. It is notable that a variety of Gaussian and linear signal processing methods have been applied frequently for spotting the Motor Imagery (MI) based EEG signals. Though, by nature, the MI linked EEG signals are not extremely Gaussian, motionless, or linear dynamical [5]. It has become essential to find a leading method that can classify specifically non-linear signals and reach the best possible output. Different kinds of artifacts cancel data recording. Thus, some preprocessing tasks are performed prior to the feature extraction to lessen the Electrooculogram (EOG) artifacts [6, 7]. It becomes more complicated to settle the multichannel or multiclass feature extraction difficulties.

The feature extraction is a vital job in a BCI as its intention is to extract mental chore related information (features) from the brain signal irrespective of the quality of the EEG signal. The likelihood of proper brain state recognition can be improved if the feature extraction unit converts the EEG signal in such a way that the signal to noise ratio (SNR) can be increased as much as possible. Since the last decade, a countless variability of features has been extracted from EEG signals and tried to design BCI, such as, band powers (BP), power spectral density (PSD) standards, autoregressive (AR) and adaptive autoregressive (AAR) parameters, Wavelet, Kalman filtering, principal component analysis, independent component analysis, common spatial pattern, and multivariate autoregressive model [8]. Among the variety of features, the frequency domain and common spatial patterns (CSP) features are popular in designing BCI. The frequency feature is based on the ERD/ERS (Event-related synchronization and desynchronization) phenomenon that is an authentic movement or motor imagery of left- or right-hand results in desynchronization of μ-band (e.g., 8-13 Hz) oscillations in the contralateral EEG along with simultaneous synchronization of central β-bands (e.g., 18-26 Hz) oscillations in the ipsilateral EEG signal [9]. The CSP feature illustrates the topographic pattern of brain rhythm modulations which is different in different motor movement imagination. Regarding the design of a BCI system, some critical aspects of these features must be considered: EEG signals have a poor signal-to-noise ratio, feature vectors are often of high dimensionality and the EEG features are not motionless since the EEG signals may promptly fluctuate over time and particularly over sessions. To deal with these factors, the proposed research work will use CSP, and higher order statistics-based features, and investigate the possibilities of adaptive CSP filter for multichannel signal processing.

Another important question in designing a BCI is interpreting the extracted features from multichannel EEG signals [10]. To achieve this goal, classification algorithms (supervised or unsupervised) are mostly used. In BCI development, the machine learning technique is used to obtain an effective classifier that can accommodate many parameters (features) to the characteristics of the user's brain signals. Till now, several classification algorithms have been used to design the BCI systems, e.g., linear classifiers (Linear Discriminant Analysis (LDA), Fisher's LDA Support Vector Machine), neural networks (Multilayer Perception-NN], Learning Vector Quantization-NN), nonlinear Bayesian classifiers (Hidden Markov Model, Bayes quadratic), nearest neighbor classifiers (k-NN, Mahalanobis distance), and combinations of classifiers [11, 12]. These algorithms are applied to detect 'patterns' of EEG features and develop a rule to identify the feature characteristic to separate into intended labels. The performance of pattern identification depends on both the extracted features and the classification technique employed [13]. In connection with feature interpretation, the primary consideration of this research work is to use the linear classification method, but other available classification techniques will also be investigated.

4. TECHNIQUES

The proposed research work is to develop an algorithm (interface) that will be consumed a human's intention of motor progress in the shape of multichannel EEG signals; and, in return, will manage (translate) the input signal to provide a control signal for an outside device. The line of the art of the proposed research work is shown in Fig. 2, and it can be described in the following steps below.

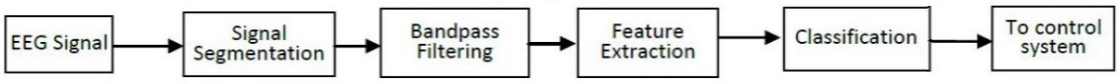

Fig. 2. Flow Diagram for Feature Extraction and Classification in a BCI

4.1 Data Acquisition and Paradigm

One of the objectives of this research work is to apply multichannel EEG signal and, hence, at least 3 channels of EEG signal will be recorded from the motor cortex area: usually C3, C4 and Cz location of EEG electrode montage. BIOPAC-MP160 amplifier with EEG (Electroencephalography) data acquisition and analysis platform with AcqKnowledge software, permitting advanced research for BCI applications and establishing acquisition of a broad range of signals and measurements. A computer-controlled thinking technique (paradigm) will be applied to record EEG signals. The paradigm will regulate up to 4 types of imagery (left, right, up and down). For any subject, multiple numbers of EEG sessions will be arranged, where some of these sessions will be used for training and validation of the interface, and the rest will be used for testing the interface with unknown EEG signals. For the online interface, the EEG signal will be acquired and processed without any paradigm.

4.2 Feature Extraction Technique

To differentiate the EEG signals in terms of any event of paradigm, several features will be extracted from the preprocessed EEG signal (usually after artifact removal and bandpass filtering). The primary aim of this research work is to extract and characterize the features related to ERD/ERS phenomenon (power spectral density due to event related desynchronization and synchronization) and the feature due to common spatial filtering [14]. In addition, the research work will look at the feature by adaptive autoregressive parameters and independent component analysis.

4.3 Classification Algorithm

Each extracted feature will be transformed and generates commands at this time of signal processing. In the training phase, feature characteristics will be assessed, and a thought identification rule will be established. The same rule will be applied in the online (evaluation) phase. The LDA classifier (Fisher's LDA) will be the primary aim to implement into BCI [15]. Besides this, Support Vector Machine and nonlinear Bayesian classifiers will be explored to achieve higher performance of the interfacing system.

4.4 Performance Measures

A microcontroller-based interfacing circuit and its code will be established, which will lead to the steps toward

an evaluation of the classification algorithm based on multichannel EEG signals. The interfacing performance will be assessed by two standard statistical measures: detection accuracy and Kohen's kappa [15]. A confusion matrix will be computed for performance measurement when compared with actual and interface assessed events in all training instances. The performance of the proposed algorithm will be compared with the same of the contemporary algorithm for the Brain Computer Interface with the subject's intention.

4.4.1. Detection Accuracy

Using the confusion matrix (CM), the left and right accuracies for each instant of the paradigm are computed by the following formulae:

$$\text{Left accuracy} = \frac{(\text{finally obtained negative in CM} \times 100)}{(\text{total number of input as left})} \quad (1)$$

$$\text{Right accuracy} = \frac{(\text{finally obtained positive in CM} \times 100)}{(\text{total number of input as right})} \quad (2)$$

The mean of left and right hand MI accuracy are called here as the overall accuracy.

4.4.2. Cohen's Kappa

Cohen's kappa is a statistical measurement that provides an index of interrater reliability. The computation of kappa at each instance begins from the CM ready by comparing the appearance of two raters: the actual events and the estimated events (observed at the classifier's output). From the definition, Cohen's kappa can be written as,

$$k = \frac{(P_0 - P_c)}{(1 - P_c)} \quad (3)$$

Where, Po means the relative observed agreement between raters and Pc for the hypothetical likelihood of chance agreement. The maximum possible value of Cohen's kappa is limited to 1 and then the raters are in complete agreement if there is no agreement among the raters, k = 0.

5. BENEFIT AND FINANCIAL IMPACT

As stated earlier, the proposed research work will deal with multichannel EEG signals processing that is related to the development of the BCI, e.g., acquisition of event-related EEG signals and feature interpretation (clustering/classification techniques) and the protocols to send messages to output devices. Since this research work will involve all issues related to signal processing which will enrich Malaysian expertise in signal processing (especially EEG processing), neuro-informatics, and rehabilitation using BCI. Disability involves hundreds of millions of families in developing countries. While the population ages, this figure is expected to rise. According to the UN Development Program (UNDP), eighty percent of people with disabilities live in developing countries. Therefore, the development of an efficient BCI for the total dysfunction of the neuromuscular system can contribute to wealth creation, enhance the quality of life and create new industries.

REFERENCES

[1] I. Lazarou, S. Nikolopoulos, P.C. Petrantonakis, I. Kompatsiaris and M. Tsolaki, "EEG-Based Brain–Computer Interfaces for Communication and Rehabilitation of People with Motor Impairment: A Novel Approach of the 21st Century, Review Article," Frontiers in Human Neuroscience, 12(14), pp. 1-18, 2018.
[2] D.D. Chakladar and S. Chakraborty, "Feature Extraction and Classification in Brain-Computer Interfacing: Future Research Issues and Challenges," Natural Computing for Unsupervised Learning, pp. 101-131, 2019.
[3] M. Jafari, T. Aflalo, S. Chivukula, S.S. Kellis, M.A. Salas, S.L. Norman, K. Pejsa, C.Y. Liu and R.A. Andersen, "The Human Primary Somatosensory Cortex Encodes Imagined Movement in the Absence of Sensory Information," Communications Biology, 3(757), pp. 1-7, 2020.
[4] S.N. Abdulkader, A. Atia and M.S.M Mostafa, "Brain Computer Interfacing: Applications and Challenges," Egyptian Informatics Journal, 16, pp. 213-230, 2015.

[5] B. Blankertz, L. Acqualagna, S. Dahne, S. Haufe, M. Schultze-Kraft, I. Stur, M. Uscumlic, M.A. Wenzel, G. Curio and M. Klaus-Robert, "The Berlin Brain-Computer Interface: Progress Beyond Communication and Control," Frontiers in Neuroscience, 10(530), pp. 1-24, 2016.
[6] R.A. Ramadan, and A.V. Vasilakos, "Brain Computer Interface: Control Signals Review," Neurocomputing, 223, pp. 26-44, 2017.
[7] A. Fernández-Rodríguez, F. Velasco-Álvarez, and R. Ron-Angevin, "Review of Real Brain-Controlled Wheelchairs," Journal of Neural Engineering, 13(6), 2016.
[8] K.S. Hong, M.J. Khan and M.J. Hong, "Feature Extraction and Classification Methods for Hybrid fNIRS-EEG Brain-Computer Interfaces," Frontiers in Human Neuroscience, 12(246), pp. 1-25, 2018.
[9] K.S. Hong, and M.J. Khan, "Hybrid-BCI Interface Techniques for Improved Classification Accuracy and Increased Number of Commands: A Review," Frontiers in Neurorobotics, 11(35), pp. 1-27, 2017.
[10] J.B. Hyun, S.K. Hyun, A. Minkyu, C. Hohyun, and A. Sangtae, "Ergonomic Issues in Brain-Computer Interface Technologies: Current Status, Challenges, and Future Direction," Computational Intelligence and Neuroscience, 2020(4876397), pp. 1-2, 2020.
[11] K. Moonyoung, C. Hohyun, W. Kyungho, A. Minkyu and C.J. Sung, "Event-related Desynchronization (ERD) May Not be Correlated with Motor Imagery BCI Performance," IEEE International Conference on Systems, Man, and Cybernetics, 2018.
[12] M.H. Alomari, E. Awada and O. Younis, "Subject-Independent EEG-Based Discrimination Between Imagined and Executed, Right and Left Fists Movements," European Journal of Scientific Research, 118(3), pp. 364-373, 2014.
[13] H. Bashashati, R.K. Ward, G.E. Birch, A. Bashashati, "Comparing Different Classifiers in Sensory Motor Brain Computer Interfaces," PLoS One 10(6), pp. 1-12, 2015.
[14] N.T.M. Huong, H.Q. Linh and L.Q. Khai, "Classification of Left/Right Hand Movement EEG Signals Using Event Related Potentials and Advanced Features," IFMBE Proceedings, 63, pp. 209-, 2018.
[15] M.R. Hasan, M.I. Ibrahimy, S.M.A. Motakabber and S. Shahid, "Classification of Multichannel EEG Signal by Linear Discriminant Analysis," Advances in Intelligent Systems and Computing, 1089, pp. 279-282, 2015.